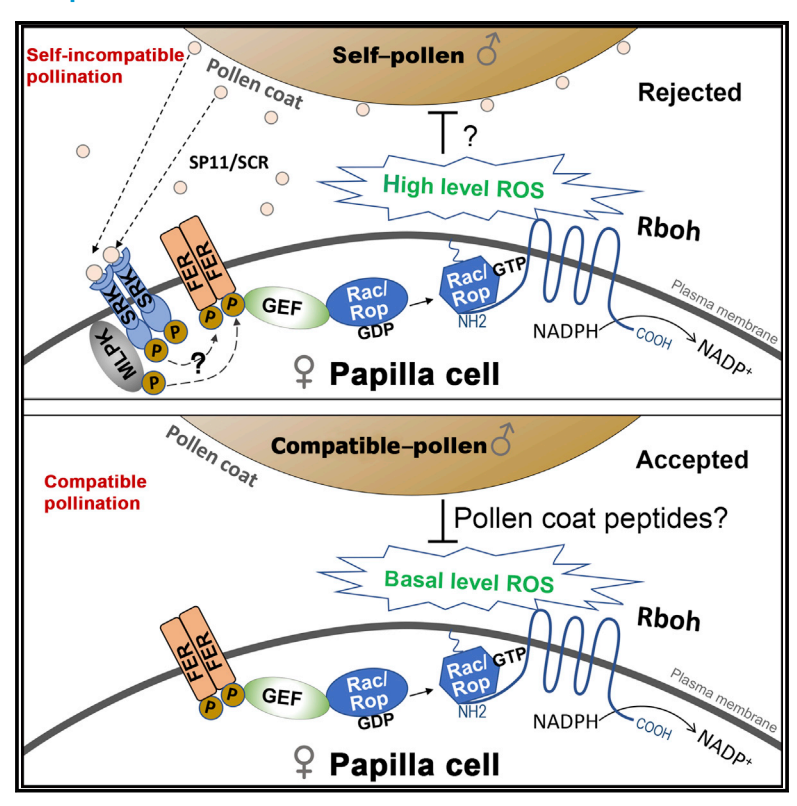
# FERONIA receptor kinase-regulated reactive oxygen species mediate self-incompatibility in *Brassica rapa*

#### **Graphical abstract**



#### **Authors**

Lili Zhang, Jiabao Huang, Shiqi Su, ..., Xiansheng Zhang, Alice Y. Cheung, Qiaohong Duan

#### Correspondence

jbhuang2018@outlook.com (J.H.), yuxiangyuan126@126.com (Y.Y.), duanqh@sdau.edu.cn (Q.D.)

#### In brief

To avoid inbreeding depressing, most plants use self-incompatibility to reject self-pollen and promote out-crossing. Zhang et al. find that self-pollination increases and compatible-pollination decreases stigmatic ROS, which are controlled via a FERONIA-Rac/Rop-Rboh module, underlying both the rejection of self-pollen and the acceptance of compatible-pollen.

#### **Highlights**

- Self-pollination increases and compatible-pollination decreases stigmatic ROS
- Reducing ROS can break down SI response
- Self-pollination-induced ROS increase is regulated by FER-Rac/Rop-Rboh module
- FER-Rac/Rop-Rboh module-dependent stigmatic ROS regulate compatible response





#### **Article**

# FERONIA receptor kinase-regulated reactive oxygen species mediate self-incompatibility in *Brassica rapa*

Lili Zhang,<sup>1,2,7</sup> Jiabao Huang,<sup>1,2,7,\*</sup> Shiqi Su,<sup>1,2,7</sup> Xiaochun Wei,<sup>4,7</sup> Lin Yang,<sup>1,2,7</sup> Huanhuan Zhao,<sup>1,2</sup> Jianqiang Yu,<sup>1,2</sup> Jie Wang,<sup>1,2</sup> Jiyun Hui,<sup>1,2</sup> Shiya Hao,<sup>3</sup> Shanshan Song,<sup>1,2</sup> Yanyan Cao,<sup>1,2</sup> Maoshuai Wang,<sup>1,2</sup> Xiaowei Zhang,<sup>4</sup> Yanyan Zhao,<sup>4</sup> Zhiyong Wang,<sup>4</sup> Weiqing Zeng,<sup>1,6</sup> Hen-Ming Wu,<sup>5</sup> Yuxiang Yuan,<sup>4,\*</sup> Xiansheng Zhang,<sup>1</sup> Alice Y. Cheung,<sup>5</sup> and Qiaohong Duan<sup>1,2,8,\*</sup>

#### **SUMMARY**

Most plants in the *Brassicaceae* evolve self-incompatibility (SI) to avoid inbreeding and generate hybrid vigor. Self-pollen is recognized by the S-haplotype-specific interaction of the pollen ligand S-locus protein 11 (SP11) (also known as S-locus cysteine-rich protein [SCR]) and its stigma-specific S-locus receptor kinase (SRK). However, mechanistically much remains unknown about the signaling events that culminate in self-pollen rejection. Here, we show that self-pollen triggers high levels of reactive oxygen species (ROS) in stigma papilla cells to mediate SI in heading Chinese cabbage (*Brassica rapa* L. ssp. *pekinensis*). We found that stigmatic ROS increased after self-pollination but decreased after compatible(CP)- pollination. Reducing stigmatic ROS by scavengers or suppressing the expression of respiratory burst oxidase homologs (Rbohs), which encode plant NADPH oxidases that produce ROS, both broke down SI. On the other hand, increasing the level of ROS inhibited the germination and penetration of compatible pollen on the stigma, mimicking an incompatible response. Furthermore, suppressing a *B. rapa* FERONIA (FER) receptor kinase homolog or Rac/Rop guanosine triphosphatase (GTPase) signaling effectively reduced stigmatic ROS and interfered with SI. Our results suggest that FER-Rac/Rop signaling-regulated, NADPH oxidase-produced ROS is an essential SI response leading to self-pollen rejection.

#### **INTRODUCTION**

To promote out-crossing and prevent inbreeding, many flowering plants utilize a genetically controlled mechanism called self-incompatibility (SI) for the selective rejection of self-incompatible pollen at the stigma surface of the female organ pistil. In the Brassicaceae, self-pollen is recognized through the Shaplotype-specific interaction of the pollen-coat encoded S-locus protein 11 (SP11)/S-locus cysteine-rich protein (SCR) peptide (SP11/SCR) and the stigma papilla cell-membrane-localized S-locus Ser/Thr receptor kinase (SRK). The recognition of self-pollen induces autophosphorylation of SRK and a signaling cascade in the papilla cells that ultimately lead to self-pollen rejection. Self-pollen rejection. Self-pollen rejection.

So far, only two proteins, the *M*-locus protein kinase (MLPK)<sup>7</sup> and ARM-repeat containing 1 (ARC1) E3 ubiquitin ligase,<sup>8</sup> have been identified as the direct downstream effectors of SRK. MLPK was identified as a positive regulator of the SI response in *Brassica rapa* (*B. rapa*), but it remains unclear how it functions and whether it is required throughout the Brassicaceae.<sup>7,9-12</sup> ARC1 is phosphorylated by SRK and targets proteins required for compatible (CP) responses for degradation, leading to the blocking of hydration and metabolic activation of self-pollen.<sup>8,13-19</sup> Efforts to introduce SI from various Brassicacea into the self-compatible *Arabidopsis thaliana*<sup>20-24</sup> suggest that more components are likely to be involved for the rejection of self-pollen during SI response in the *Brassica* family plants.

Reactive oxygen species (ROS) are known to play important roles in diverse physiological processes, <sup>25–33</sup> including pollen tube growth. <sup>25,27,34</sup> Many flowering plants constitutively

<sup>&</sup>lt;sup>1</sup>State Key Laboratory of Crop Biology, College of Horticulture Science and Engineering, Shandong Agricultural University, Tai'an, 271018 Shandong, China

<sup>&</sup>lt;sup>2</sup>College of Horticulture Science and Engineering, Shandong Agricultural University, Tai'an, 271018 Shandong, China

<sup>&</sup>lt;sup>3</sup>School of Arts and Sciences, Rutgers University, New Brunswick, NJ 08901, USA

<sup>&</sup>lt;sup>4</sup>Institute of Horticulture, Henan Academy of Agricultural Sciences, Zhengzhou, 450002 Henan, China

<sup>&</sup>lt;sup>5</sup>Department of Biochemistry and Molecular Biology, Molecular Cell Biology and Plant Biology Programs, University of Massachusetts, Amherst, MA 01003, USA

<sup>&</sup>lt;sup>6</sup>Present address: Trait Discovery, Corteva Agriscience, Johnston, IA 50131, USA

<sup>&</sup>lt;sup>7</sup>These authors contributed equally

<sup>&</sup>lt;sup>8</sup>Lead contact

<sup>\*</sup>Correspondence: jbhuang2018@outlook.com (J.H.), yuxiangyuan126@126.com (Y.Y.), duanqh@sdau.edu.cn (Q.D.) https://doi.org/10.1016/j.cub.2021.04.060



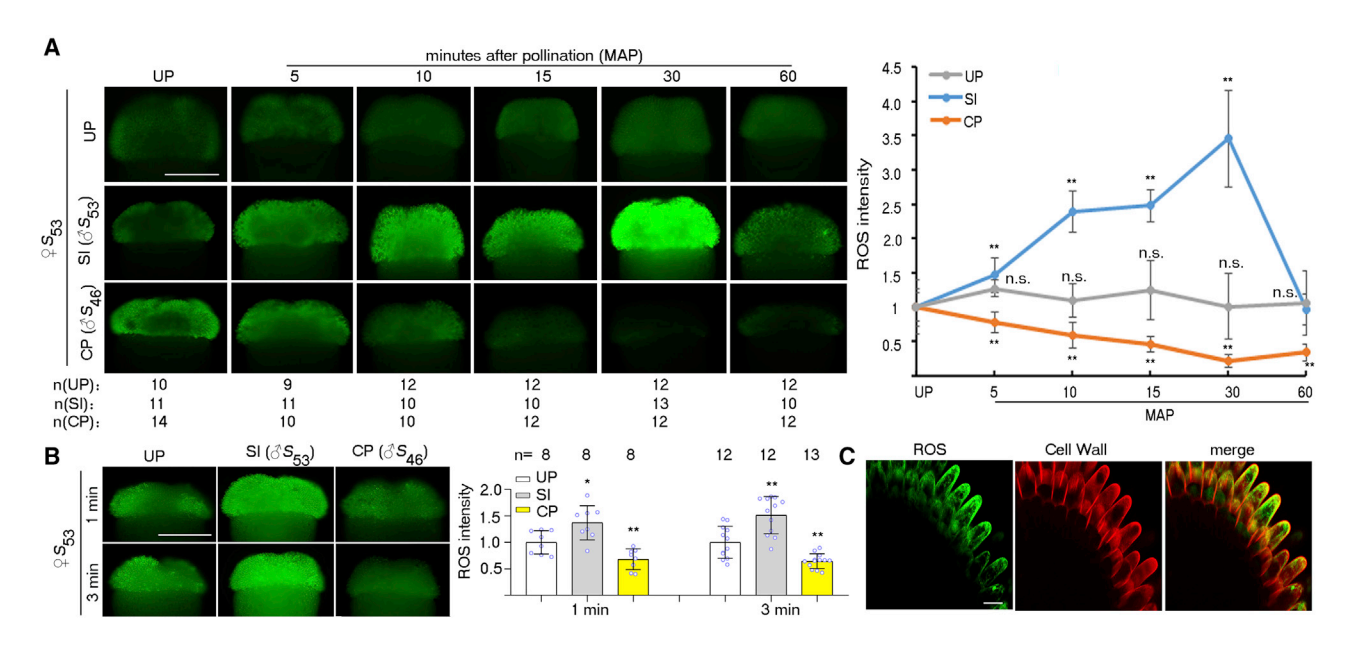


Figure 1. Stigmatic ROS increase after self-pollination and decrease after compatible-pollination

(A and B) Stigmatic ROS. Unpollinated (UP), SI-pollinated, or CP-pollinated stigmas, stained with H2DCFDA, if not specified. Average ROS signals were measured in ImageJ; ROS in control stigmas were set at 1 for comparative analyses. Unless otherwise indicated, bar graphs or line graphs denote the mean, ±SD for all stigmatic ROS data and ± SEM for all the pollen tube growth data. Dots indicate each data point. n denotes the numbers of stigmas. Asterisks or n.s. directly above the data bars indicate significant difference (two-tailed t test; \*p < 0.05; \*\*p < 0.01) or no significant difference compared with the data bar on the far left, although \*\* or n.s. above the brackets show comparisons between the data bars as indicated. Each experiment was repeated at least three times with consistent results

(C) Co-imaging of ROS with the PI-stained cell wall in papilla cells. Scale bars in (A) and (B), 500  $\mu m$ ; (C), 10  $\mu m$ . See also Figure S1.

accumulate more ROS in mature than bud-stage stigmas, 35-38 suggesting a potential involvement of ROS in pollen-stigma interactions. It was reported that high concentrations (between 40 mM and 100 mM) of the ROS inhibitor N-acetyl-L-cysteine (NAC) completely abolished stigmatic ROS in ornamental kale (B. oleracea var. acephala), but self-pollen was still rejected. However, the treatment condition also drastically blocked compatible pollen attachment and germination,<sup>38</sup> rendering a clear conclusion for ROS involvement in SI or CP response impossible.

In this study, we examined stigmatic ROS during SI and CP responses in heading Chinese cabbage (B. rapa L. ssp. pekinensis), an important vegetable crop in which SI is widely utilized to produce hybrid seeds.<sup>39</sup> We found that stigmatic ROS increase after self-pollination and decrease after compatible-pollination. Manipulating stigmatic ROS had strong impacts on pollen germination and tube growth in both SI and CP responses. These ROS-mediated responses are NADPH oxidase-dependent and controlled by B. rapa FERONIA receptor kinase (FER)-Rac/Rop signaling. Our results establish that FER-regulated stigmatic ROS increase is crucial for the SI response of the Brassicaceae.

#### **RESULTS**

#### Stigmatic ROS increase after self-pollination and decrease after compatible-pollination

To determine whether ROS are involved in the SI response of the Brassicaceae, we stained Chinese cabbage stigmas at different time points after SI or CP pollination, with the general ROS probe 2',7'-dichlorodihydrofluorescein diacetate (H<sub>2</sub>DCFDA).<sup>26,28,40,41</sup>

Compared with the steady-state level of ROS in unpollinated (UP) stigmas (Figure 1A), ROS started to show significant increase as early as 1 min after self-pollination and reached the maximum level, about 3-fold that of unpollinated stigmas, within 30 min (Figures 1A and 1B). To the contrary, ROS was notably reduced by 5 min after compatible-pollination and continued to decrease within 60 min after pollination (MAP) (Figures 1A and 1B), consistent with the time course of SI and CP responses (Figures S1A-S1C). Co-staining stigmas with H<sub>2</sub>DCFDA and the cell wall indicator propidium iodide (PI) showed that ROS was located in the cytoplasm of papilla cells, near the periphery of the plasma membrane (Figure 1C). Similar changes of ROS after SI or CP responses were also observed in stigmas stained with two other often-used ROS probes, hydroxyphenyl fluorescein and dihydroethidium, and in stigmas from two other cultivars, DHB848 and R16, but not in mechanically stressed stigmas (Figures S1E-S1I). These results suggest that the increase and decrease of stigmatic ROS is a specific response induced by SI and CP, respectively.

#### The increase of stigmatic ROS after self-pollination is S-haplotype specific

To explore the molecular mechanism of the stigmatic ROS increase after self-pollination, we suppressed the expression of SRK to reduce SP11/SCR-triggered signaling and then examined the change of ROS. Efficient transformation of heading Chinese cabbage is still difficult to accomplish, but antisense oligodeoxyribonucleotide (AS-ODN) has been used successfully to suppress target genes in pollen tubes 42-46 and in stigmas. 47,48 Because

Article



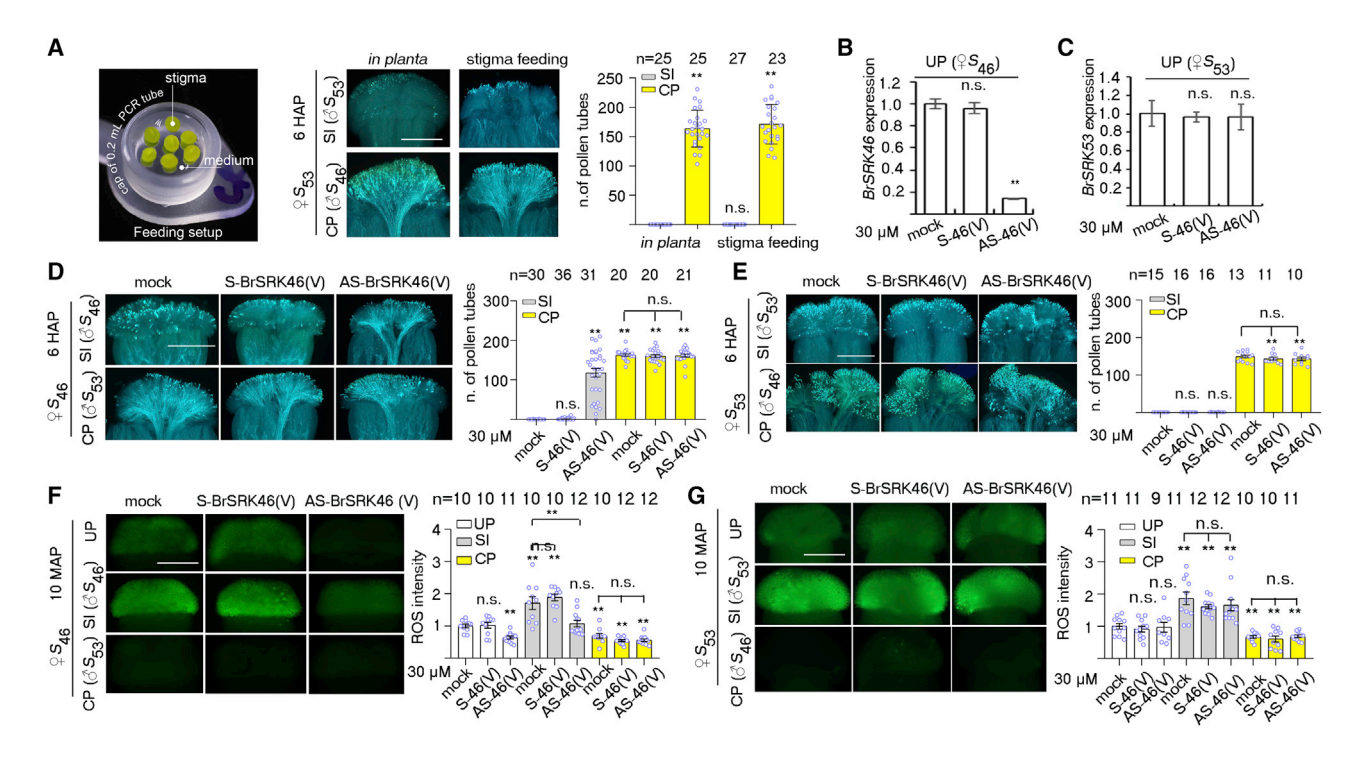


Figure 2. The increase of stigmatic ROS after self-pollination is S-haplotype specific (A) Stigmas in feeding assays maintain typical SI and CP phenotypes. (B and C) qRT-PCR analysis of BrSRK46 in S46 stigmas or BrSRK53 in S53 stigmas treated with S- or AS-BrSRK46 (V). (D and E) Aniline blue staining showing the growth of self- or compatible-pollen in S46 (D) or S53 stigmas (E) with S- or AS-BrSRK46(V) treatment.

(F and G) ROS of S<sub>46</sub> (F) or S<sub>53</sub> stigmas (G) with S- or AS-BrSRK46(V) treatment, before and after SI or CP. Scale bars, 500 μm. Detailed statistical analysis methods are shown in the STAR Methods.

See also Figure S2.

the hypervariable region of SRK (SRK(V)) is important for the interaction specificity between SP11/SCR and SRK,4 we treated S46 (cultivar 14CR) or S<sub>53</sub> (cultivar ZY15) stigmas with S- or AS-BrSRK46(V) to specifically target BrSRK46 and S- or AS-BrSRK46(C) to target the conserved region of BrSRK46 and BrSRK53 (Figure S2A), as confirmed by quantitative RT-PCR analysis (Figures 2A-2C, S2B, and S2C). AS-BrSRK46(V) treatment specifically broke down SI of S<sub>46</sub> stigmas, but not that of S<sub>53</sub> stigmas, as demonstrated by bundles of self-pollen tubes penetrating  $S_{46}$  stigmas, but not  $S_{53}$  stigmas (Figures 2D and 2E). However, AS-BrSRK46(C) treatment significantly weakened SI of both S<sub>46</sub> stigmas and  $S_{53}$  stigmas (Figures S2D and S2E). In contrast, neither of the above treatments impacted the growth of compatible-pollen tubes (Figures 2D, 2E, S2D, and S2E). AS-BrSRK46(V) treatment also specifically reduced ROS of unpollinated S<sub>46</sub> stigmas as well as suppressed the increase of ROS triggered by self-pollination (Figure 2F) but did not affect ROS of S<sub>53</sub> stigmas before and after self-pollination (Figure 2G). However, AS-BrSRK46(C) treatment significantly reduced ROS of both S<sub>46</sub> stigmas and  $S_{53}$  stigmas, before and after self-pollination (Figures S2G and S2H). In contrast, S-BrSRK46(V)- or S-BrSRK46(C)treated S<sub>46</sub> stigmas and S<sub>53</sub> stigmas maintained typical SI phenotypes and similar levels of ROS to mock-treated stigmas (Figures 2D-2G and S2D-S2H). These results strongly support that both the ROS production in unpollinated stigmas and the increase of stigmatic ROS levels after self-pollination depend on functional SRK.

#### High levels of stigmatic ROS are essential to reject selfpollen

We then tested whether self-pollen-induced stigmatic ROS increase is essential for self-pollen rejection. Stigmas were pretreated with different concentrations of ROS scavengers. CuCl<sub>2</sub>, Tiron, KI, or sodium benzoate, and then self- or compatible-pollinated. Results established that these scavengers all effectively reduced the stigmatic ROS levels before and after self-pollination (Figures 3A and S3A-S3C), and they significantly weakened or completely broke down SI in a dose-dependent manner, as demonstrated by the increasing number of self-pollen tubes in scavenger-treated stigmas (Figures 3A and S3B). Importantly, and contrary to 100 mM NAC treatment in Lan et al.,38 ROS scavengers at the indicated concentrations did not inhibit compatible-pollen growth (Figures 3A and S3B), indicating the stigma and pollen viability was not affected. Taken together, these results demonstrated unambiguously that the increase of stigmatic ROS is essential for self-pollen rejection.

Next, we speculated that the rapid induction of high ROS levels after self-pollination is utilized to arrest self-pollen, similar to the ROS burst in a wide range of plant-pathogen interactions to inhibit the invading pathogens. 49-54 To prove this, we carried out a "stigma transfer experiment" (Figure S3D) by first pollinating stigmas with self-pollen for 0-60 min to induce different levels of ROS elevation and then transferring them onto 3 mM CuCl<sub>2</sub> medium for further cultivation. Compared to the typical SI phenotypes in stigmas that were not transferred, an average



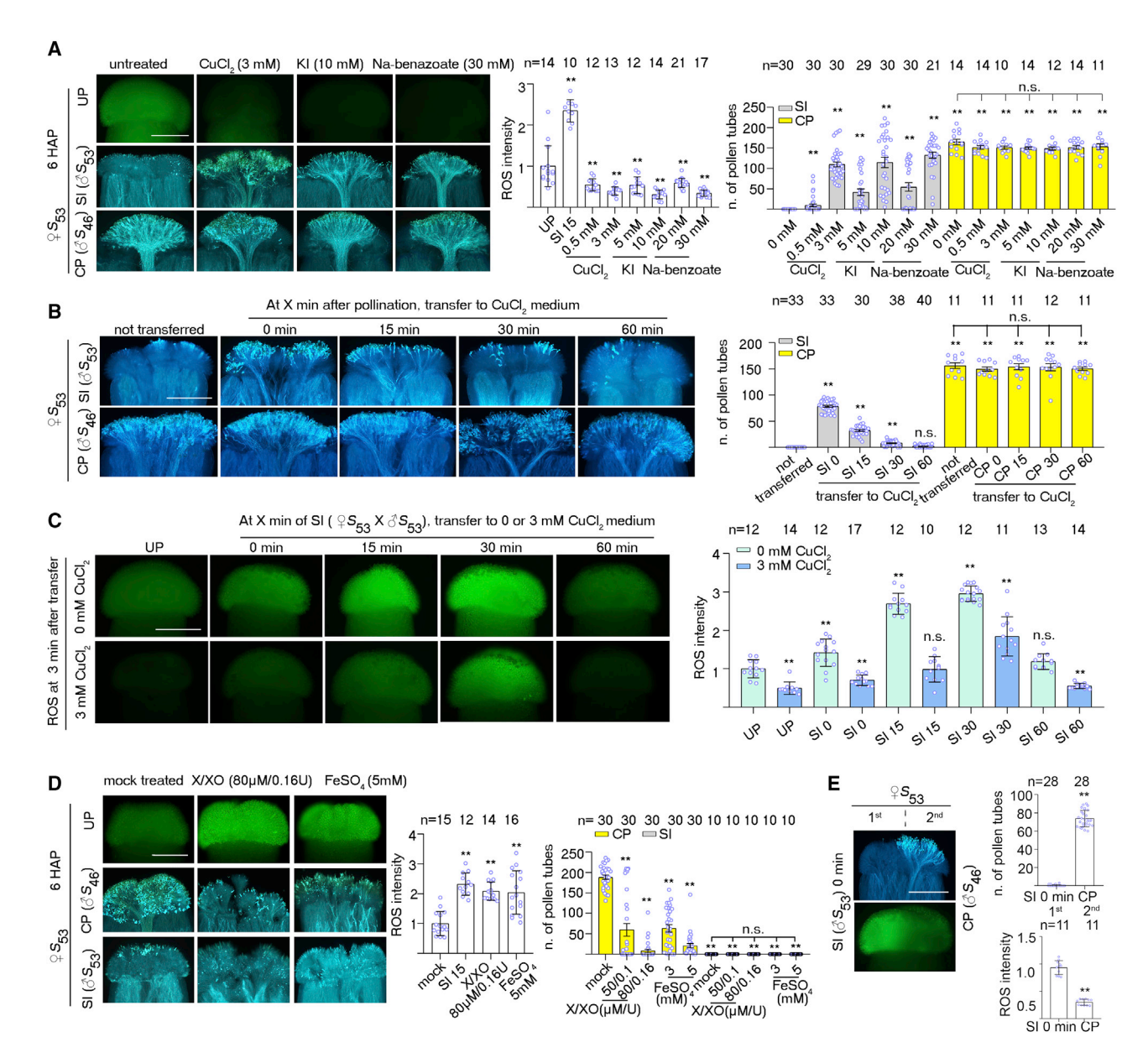


Figure 3. High levels of stigmatic ROS are essential to reject self-pollen

- (A) ROS and the growth of self- or compatible-pollen in scavenger-treated stigmas.
- (B and C) The growth of self- or compatible-pollen (B) and stigmatic ROS (C) in stigmas transferred to CuCl2-medium after SI.
- (D) ROS and the growth of self- or compatible-pollen in stigmas with applied ROS.
- (E) Pollen growth and ROS in dual self- or compatible-pollinated stigmas. Scale bars, 500 μm. Detailed statistical analysis methods are shown in the STAR Methods.

See also Figure S3.

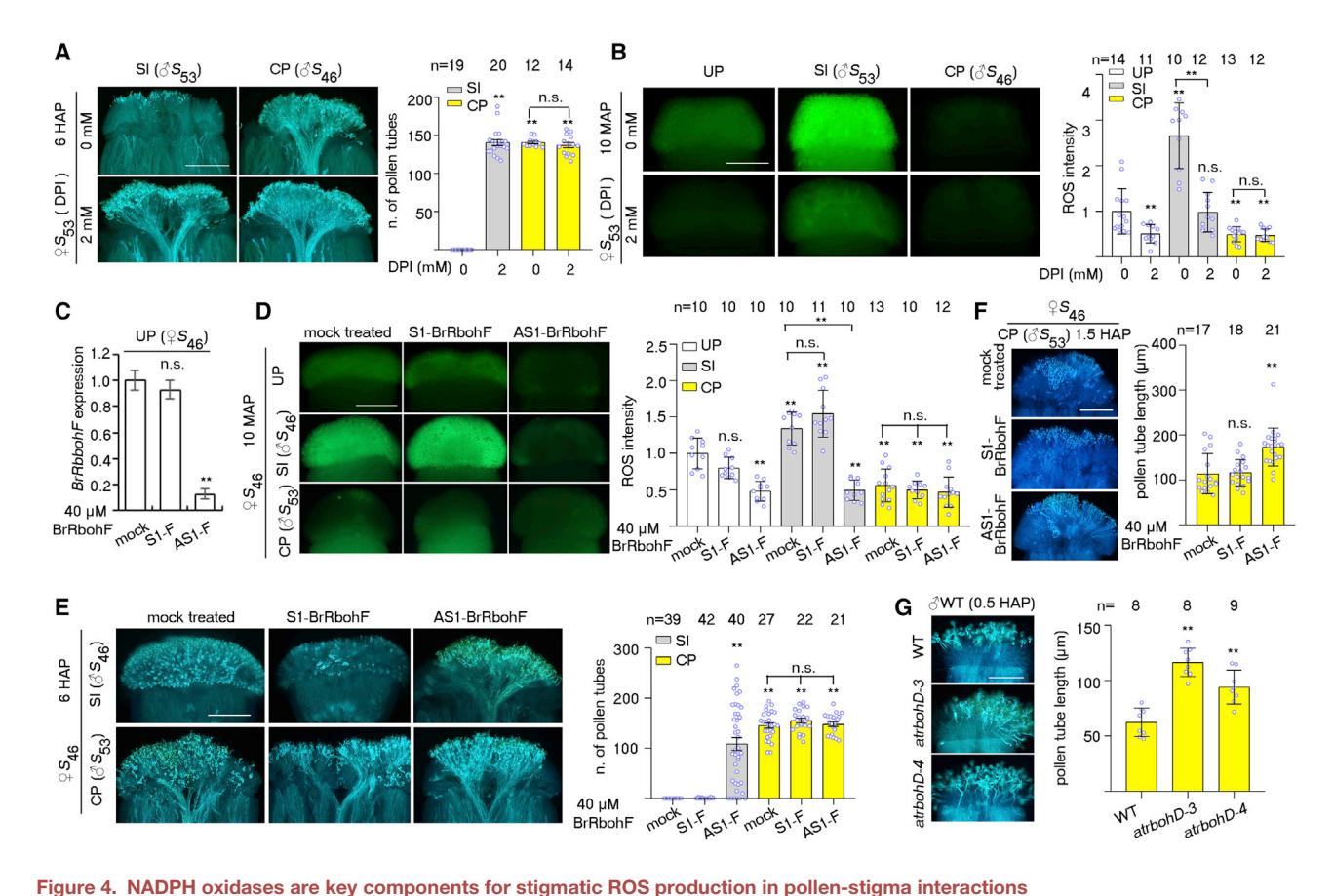
of 80 self-pollen tubes were salvaged and grew into the SI 0 stigmas, which were immediately transferred after self-pollination, but only 42 and 10 self-pollen tubes grew into the SI 15 and SI 30 stigmas (Figures 3B and S3F). These results correlated with ROS of SI 0, SI 15, SI 30, and SI 60 stigmas were all significantly reduced at 3 min after transferring onto 3 mM CuCl<sub>2</sub> medium, compared to those onto 0 mM CuCl<sub>2</sub> (Figures 3C and S3E). In contrast, growth of compatible-pollen tubes was not affected in comparably treated stigmas (Figure 3B). Although ROS returned to a lower level in SI 60 stigmas (Figure 3C), no self-pollen

tubes were salvaged (Figures 3B and S3F), possibly because prolonged exposure to high levels of ROS had irreversibly arrested the self-pollen grains on the stigma.

We also investigated whether high levels of ROS are inhibitory to compatible pollen. When xanthine/xanthine oxidase (X/XO) or FeSO<sub>4</sub> (Fe<sup>2+</sup>-mediated Fenton reaction) were applied onto the stigma, they generated ROS to a level comparable to that in SI 15 stigmas (Figures 3D and S3G) and inhibited compatible-pollen (Figure 3D). These results therefore suggest that ROS have a general, non-selective, inhibitory effect on pollen.

**Article** 





(A and B) The growth of self- or compatible-pollen and ROS in stigmas with DPI treatment.

(C-E) The effect of S1- or AS1-BrRbohF treatment on BrRbohF expression (C), ROS (D), and the growth of self- or compatible-pollen (E).

(F) The length of compatible-pollen tubes at 1.5 HAP (F) in stigmas treated with S1- or AS1-BrRbohF.

(G) The growth of wild-type (WT) pollen tubes at 0.5 HAP in Arabidopsis (compatible cruciferous plant) atrbohD-3 and atrbohD-4 T-DNA mutant stigmas. Scale bar in (G), 100 μm; others, 500 μm. Detailed statistical analysis methods are shown in the STAR Methods. See also Figures S4 and S5.

#### Self- and compatible-pollen trigger local changes in stigmatic ROS status

We also examined the change of ROS in dual self- and compatible-pollination on a single stigma, mimicking a natural pollination. Consistent with a previous report, 21 dual self- and compatible-pollinations at the same time (0 min) or 15 min apart both showed the absence of self-pollen tubes at the SI half and bundles of compatible-pollen tubes penetrating the CP half of each stigma (Figures 3E and S3H). Moreover, both self- and compatible-pollination elicited their typical stigmatic responses, resulting in higher levels of ROS at the SI half and lower levels of ROS at the CP half (Figures 3E and S3H). Consistently, significantly higher or lower levels of ROS were also observed at the SI half or the CP half, respectively, than the unpollinated half of each stigma in these assays (Figure S3I). Together, our results imply that, in a natural pollination process, when a stigma encounters a mix of self- and compatible-pollen grains, the induced local increase or decrease of ROS would arrest self-pollen but allow compatible-pollen in the vicinity to germinate.

#### NADPH oxidases are key ROS-producing enzymes in SI reaction

NADPH oxidases are involved in ROS production and conserved across animals, fungi, and plants. 49,55 To examine the involvement of NADPH oxidases in the ROS production during pollen-stigma interactions, we treated stigmas with diphenyleneiodonium chloride (DPI), a common inhibitor for NADPH oxidases.<sup>26,28</sup> We found that pretreatment with 2 mM DPI followed by stigma transfer to basic PGM allowed the growth of self-pollen tubes into the stigma (Figures 4A, S4A, and S4B) although not affecting compatible-pollen (Figures 4A, S4A, and S4B). Furthermore, 2 mM DPI treatment was adequate to reduce ROS before pollination and also blocked the ROS increase after self-pollination (Figure 4B). However, overdose or prolonged DPI treatment inhibited the growth of both SI and CP pollen (Figures S4A and S4B). Together, these results demonstrate that NADPH oxidases are the prime candidate enzymes involved in producing ROS during pollen-stigma interactions.

Among the 13 NADPH-oxidase-encoding genes in B. rapa genome,56-58 (B. rapa RESPIRATORY-BURST OXIDASE HOMOLOGs, BrRbohs) BrRbohD1, BrRbohD2, BrRbohF, and BrRbohl were the most abundantly expressed in the stigma (Figure S4C). Similar to that in Arabidopsis, 49,55 BrRbohs showed plasma membrane localization in agro-infiltrated tobacco leaves (Figure S4D). AS1-BrRbohF treatment, not mock or S1-BrRbohF, dramatically reduced the abundance of BrRbohF transcript, reduced ROS before pollination, and



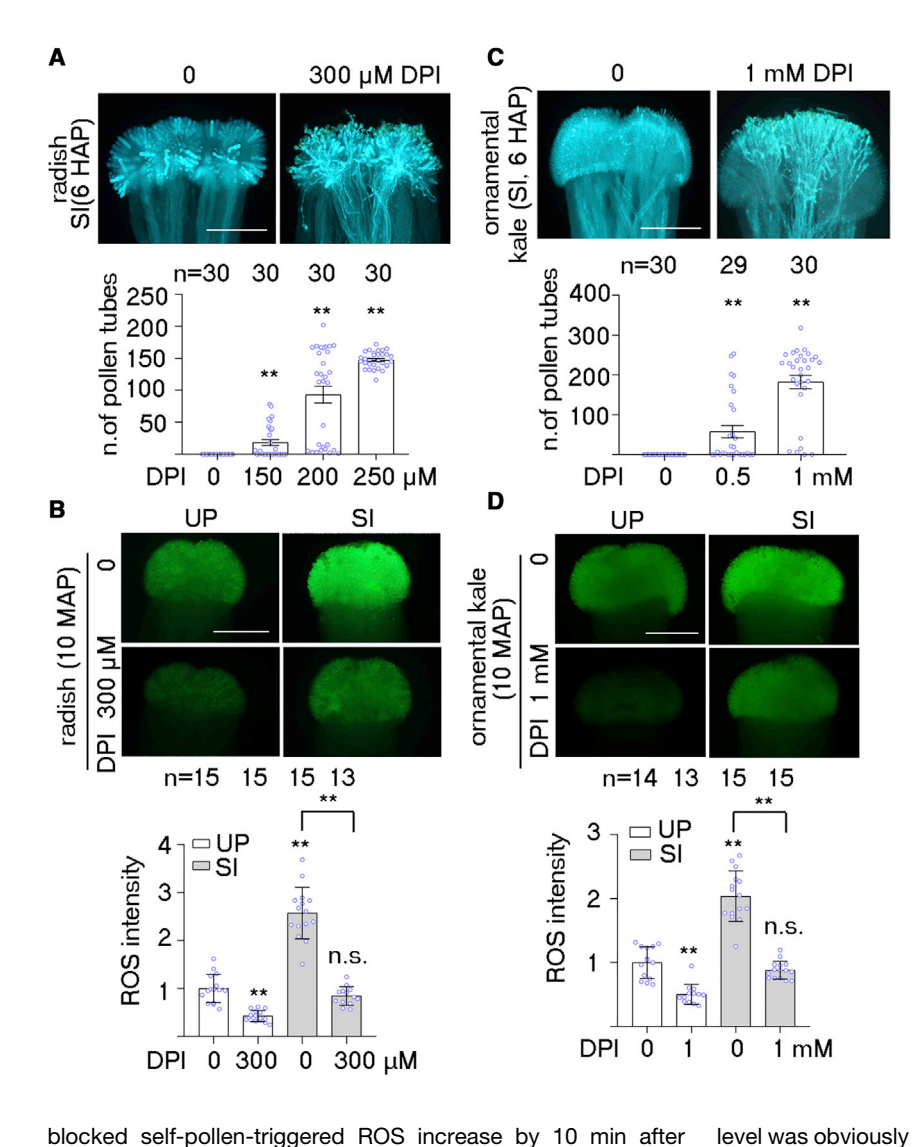


#### Figure 5. The involvement of NADPH-oxidase-dependent stigmatic ROS in the SI response of other Brassica species

(A and B) The growth of self-pollen (A) and ROS before and after SI (B) in radish stigmas treated with

(C and D) The growth of self-pollen (C) and ROS before and after SI (D) in ornamental kale stigmas treated with DPI. Scale bars, 500 µm. Detailed statistical analysis methods are shown in the STAR Methods

#### **NADPH** oxidase-dependent stigmatic ROS regulate compatible pollen growth

The accumulation of ROS35-38 and defense-related proteins<sup>38</sup> in mature stigmas of many angiosperms suggests that basal levels of stigmatic ROS, believed to be associated with defending the reproductive parts against pathogen attacks, might also have inhibitory effect on compatible pollination. We found that compatible-pollen tubes in AS1-BrRbohF-treated stigmas were significantly longer than that in mock or S1-BrRbohF-treated stigmas at 1.0 or 1.5 HAP (Figures 4F and S4H), suggesting that reducing the basal ROS level promotes the growth of compatible pollen. To further study the effect of ROS on the growth of compatible pollen, we utilized Arabidopsis thaliana, which is a typical compatible cruciferous model plant<sup>21,59-61</sup> and has abundant mutant resources. 62 ROS in Arabidopsis stigmas were DPI sensitive (Figure S5A), and their

level was obviously reduced after pollination, but not responsive to mechanical stress (Figures S5B and S5C). RbohD is widely expressed and mediates diverse functions in many plant species. 49,55 Two independent transfer DNA (T-DNA) insertional mutant alleles for RbohD, rbohD-3 or rbohD-4, showed significantly lower levels of ROS compared to that in wild-type stigmas before and after pollination (Figures S5D-S5G). Furthermore, pollen tubes in rbohD-3 or rbohD-4 mutant stigmas were significantly longer than that in wild-type stigmas at 0.5 or 1.0 HAP (Figures 4G and S5H). Together, these results suggest that NADPH oxidases are key ROS-producing enzymes for maintaining basal ROS in unpollinated stigmas and they are suppressed during CP reactions to facilitate pollen tube growth but are induced during SI reactions to arrest self-pollen.

#### with AS-ODN against BrRbohD1, BrRbohD2, and BrRbohl all reduced the expression of the corresponding target genes, suppressed the levels of stigmatic ROS, and weakened the strength of SI (Figures S4I-S4M). Although there was some cross-suppression of other BrRboh homologs with each of the AS-ODNs (Figures S4N and S4O), our results nevertheless support that the four BrRboh genes have redundant functions in ROS production during the SI response.

self-pollination (Figures 4C and 4D). Importantly, AS1-BrRbohF

effectively broke down SI and promoted the growth of self-pol-

len tubes in an AS-ODN-concentration-dependent manner

without notable impacts on the growth of compatible-pollen

tubes (Figures 4E and S4E-S4G). Furthermore, treatments

To investigate the involvement of ROS during SI responses of other cruciferous plants, we treated radish (Raphanus sativus) and ornamental kale (B. oleracea var. acephala) stigmas with DPI. These DPI-treated stigmas showed the breakdown of SI (Figures 5A and 5C) and the reduction of ROS before and at 10 min after self-pollination (Figures 5B and 5D), indicating that NADPH-oxidase-regulated ROS production could be a common strategy adopted by the Brassicaceae to reject self-pollen.

#### NADPH oxidases are regulated by Rac/Rop signaling during pollen-stigma interactions

Furthermore, NADPH oxidase activity was found significantly increased or decreased at 5, 10, and 15 min after self- or compatible-pollination, respectively, compared to that in unpollinated stigmas (Figure 6A), suggesting that NADPH oxidase activity is tightly controlled in pollen-stigma interactions. Rac/Rop

#### **Article**



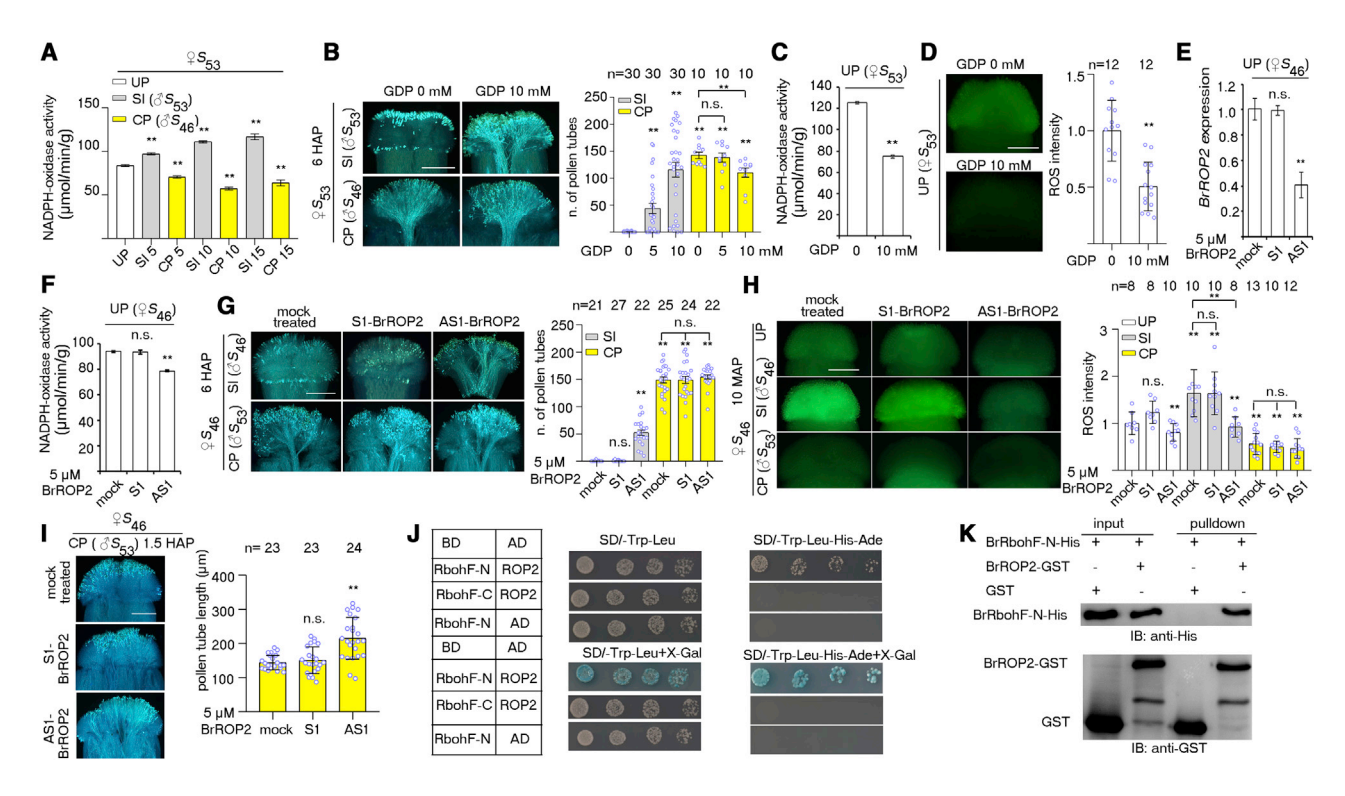


Figure 6. NADPH-oxidase-dependent ROS production during pollen-stigma interaction is mediated by Rac/Rop GTPases (A) NADPH-oxidase activity in UP, SI, or CP stigmas.

(B-D) The growth of self- or compatible-pollen (B), NADPH oxidase activity (C), and ROS (D) in GDP-treated stigmas.

(E-H) The effect of S1- or AS1-BrROP2 treatment on BrROP2 expression (E), NADPH oxidase activity (F), the growth of self- or compatible-pollen (G), and ROS

(I) The length of compatible-pollen tubes at 1.5 HAP in stigmas with S1- or AS1-BrROP2 treatment.

(J and K) N-terminal of BrRbohF (BrRbohF-N), not the C-terminal of BrRbohF (BrRbohF-C), interacts with BrROP2 in yeast two-hybrid assays (J) and pull-down assays (K). Scale bars, 500 µm. Detailed statistical analysis methods are shown in the STAR Methods. See also Figure S6.

guanosine triphosphatases (GTPases), intracellular molecular switches that quickly convert between the guanosine diphosphate (GDP)-bound inactive form and the GTP-bound active form, 63 are well-established regulators of NADPH oxidases in various plant systems. 64-66 Treating stigmas with GDP, which shifts Rac/Rops to be predominantly the inactive form, drastically weakened the strength of SI without affecting compatiblepollen (Figure 6B). GDP treatment also inhibited NADPH oxidase activity (Figure 6C) and reduced ROS in the stigma (Figure 6D). These results together are consistent with Rac/Rop GTPases being important regulators of NADPH-oxidase-dependent ROS production during the SI responses.

We further identified BrROP2 as the most highly expressed ROP in the stigma among all the tested Rac/Rop GTPase-encoding genes in B. rapa (Figure S6A). AS1-BrROP2 treatment effectively reduced the transcript of BrROP2 (Figure 6E) and inhibited NADPH oxidase activity in the stigma (Figure 6F). This treatment also promoted the growth of self-pollen tubes without affecting the growth of compatible-pollen tubes into the stigmas (Figures 6G, S6B, and S6C). In contrast to the ROS increase in mock- or S1-BrROP2-treated stigmas, AS1-BrROP2-treated stigmas showed significantly reduced ROS before and at 10 min after self-pollination (Figure 6H). Consistent with our finding that reducing ROS before pollination released the inhibitory effect on the growth of compatible pollen (Figures 4F and 4G), compatible-pollen tubes in AS1-BrROP2-treated stigmas were also longer than that in mock or S1-BrROP2-treated stigmas at 1.0 HAP or 1.5 HAP (Figures 6I and S6D). Moreover, results from yeast two-hybrid and protein pull-down assays both showed direct interactions between BrROP2 and BrRbohF proteins (Figures 6J and 6K), consistent with Rac/ROP GTPases regulating the activity of NADPH oxidases through direct proteinprotein interaction. 64,65,67 These results suggest that BrROP2regulated activation of BrRbohF underlies the rapid increase of stigmatic ROS during SI response as well as the maintenance of basal ROS in unpollinated stigmas.

#### **BrROP2-regulated ROS production functions** downstream of FER signaling during pollen-stigma interactions

FER receptor kinase functions as cell surface receptor for Rac/ Rops.<sup>26</sup> We therefore examined whether FER regulates the ROS production and pollen tube growth in the stigma. Arabidopsis transgenic plants containing FER<sub>pro</sub>:FER-GFP confirmed that FER-GFP co-localized with the membrane indicator FM4-64 at the plasma membrane of the stigmatic papilla cells (Figures S7A and S7B).<sup>26,68</sup> Knockout mutations in FER, for example, fer-4<sup>26,28</sup> and sirène (srn), 69 led to the reduction of ROS before



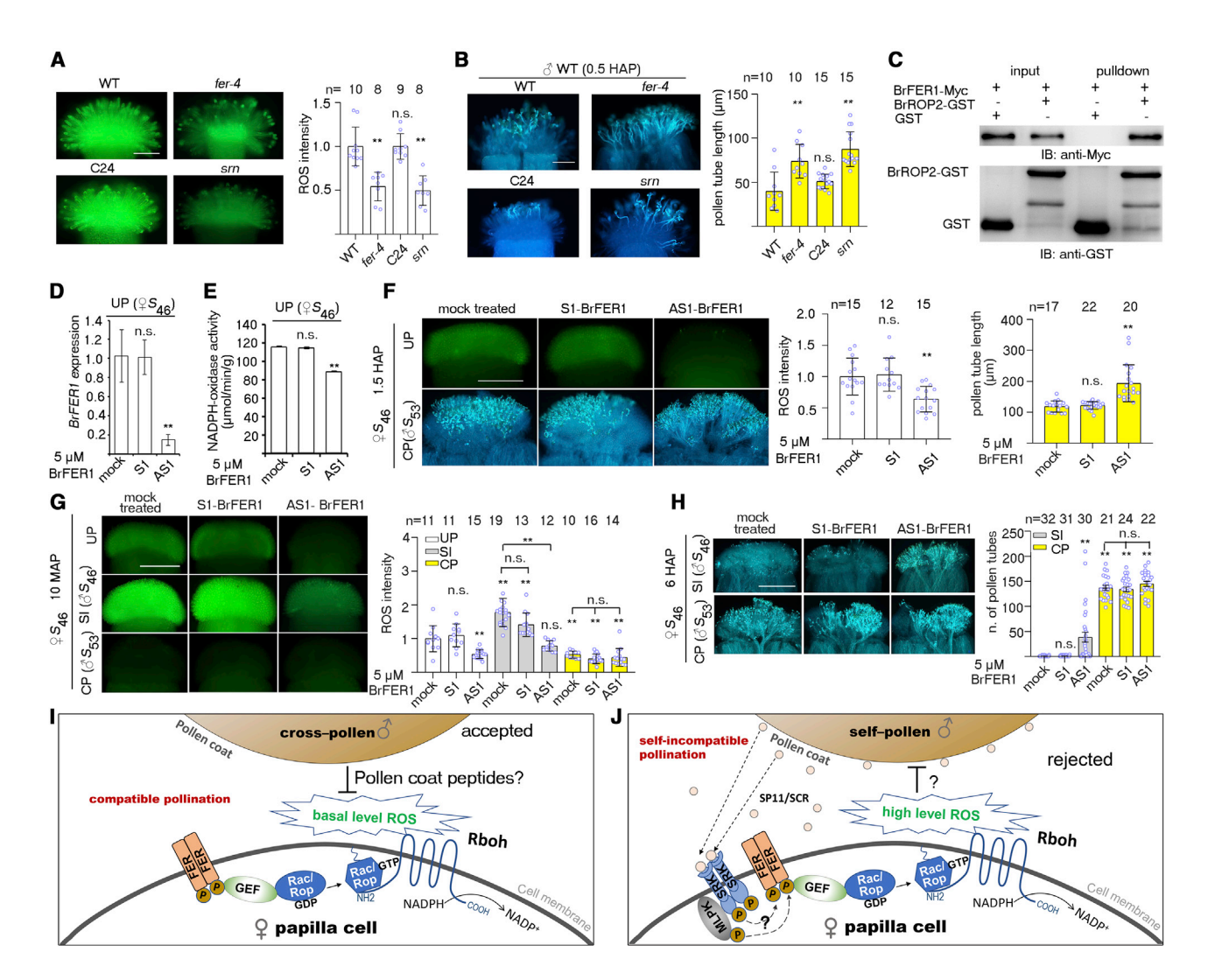


Figure 7. FERONIA-Rac/Rop signaling controls stigmatic ROS during pollen-stigma interaction

(A and B) ROS (A) and the growth of wild-type pollen tubes (B) in two alleles of Arabidopsis FER mutant stigmas, fer-4 and srn (in ecotype C24). (C) BrROP2 interacts with BrFER1 in pull-down assays.

(D and E) The effect of S1- or AS1-BrROP2 treatment on BrROP2 expression (D) and NADPH oxidase activity (E).

(F) ROS and the growth of compatible-pollen tubes at 1.5 HAP in S1- or AS1-BrFER1-treated stigmas.

(G and H) ROS (G) and the growth of self- or compatible-pollen tubes (H) in S1- or AS1-BrFER1-treated stigmas.

Scale bars in (A) and (B), 100 µm; others, 500 µm. Detailed statistical analysis methods are shown in the STAR Methods.

(I and J) Model for the FER-Rac/Rop signaling-Rboh module-regulated ROS production during SI response and CP response in Chinese cabbage. In summary, FER-Rac/Rop signaling-Rboh module mediates the basal level of ROS in mature stigmas before pollination but is downregulated by compatible-pollen to facilitate compatible-pollination (I). After pollination with self-pollen, SP11/SCR-stimulated signaling pathways could directly or indirectly result in the activation of FER-Rac/Rop signaling-Rboh module to promote the generation of high levels of ROS, leading to self-pollen rejection (J). Our results show that the ROS increase is S-haplotype specific, suggesting potential SP11/SCR-triggered SRK signaling mediates the FER-regulated response. The nature of compatible-pollen trigger in B. rapa remains to be determined; it is possible that pollen coat proteins 70,71 could be involved. Molecular interactions between the SCR/SRK signaling pathway and FER remain to be investigated. Dash lines and ? indicate "to be determined." See also Figure S7.

and after pollination, compared to that in wild-type stigmas (Figures 7A and S7C). Furthermore, wild-type pollen tubes growing in fer-4 and srn mutant stigmas were significantly longer than those in wild-type stigmas at 0.5 or 1.0 HAP (Figures 7B and S7D), implying that FER-regulated ROS in unpollinated stigmas are inhibitory to early growth of pollen on the stigma.

We further tested whether suppressing the expression of B. rapa FER homologs would affect pollen-stigma interactions in Chinese cabbage. Three Arabidopsis FER homologs were identified in B. rapa (Figure S7E). BrFER1, the only full-length FER protein (Figure S7E), functioned in the same complex together with BrROP2 by protein pull-down assays (Figure 7C). AS1-BrFER1 treatment, which effectively suppressed its expression (Figures 7D and S7F), significantly inhibited the activity of NADPH oxidases (Figure 7E) and reduced ROS of unpollinated stigmas (Figure 7F). Furthermore, AS1-BrFER1 treatment

#### **Article**



promoted the growth of compatible-pollen tubes at 1.0 or 1.5 HAP (Figures 7F and S7G), suggesting that the basal levels of ROS in unpollinated stigmas from Chinese cabbage or Arabidopsis are regulated by FER signaling and play an inhibitory role for pollen tube growth during the compatible responses.

Next, we tested whether suppressing BrFER1 influences the ROS production triggered by self-pollination and interferes with SI in Chinese cabbage. AS1-BrFER1 treatment completely abolished the self-pollen-triggered ROS increase (Figure 7G) and significantly weakened the SI response, with an average of ~50 self-pollen tubes grown into the stigmas although not noticeably impacting the CP response (Figures 7H and S7H). Interestingly, considerably lower concentrations of AS-BrFER1 (Figures 7 and S7; 5  $\mu$ M) and AS-BrROP2 (Figures 6 and S6; 5  $\mu$ M) were needed to break down SI than that of AS-BrRbohs (Figures 4 and S4; 40 μM), likely reflecting relatively high level of Rboh expression from multiple genes during SI responses. Taken together, these results support that the FER-Rac/Rop GTPase-Rboh signaling module mediates rapid ROS production during SI responses and is also important for maintaining the basal levels of ROS in unpollinated stigmas.

#### **DISCUSSION**

ROS play important roles during development and responses to external stimuli. 26,28,31,49 in angiosperms, such as A. thaliana and B. oleraceae, they accumulate to considerably higher levels in the mature stigmas than in bud stage stigmas. 35-38 Our study here demonstrates that, in heading Chinese cabbage, the FER-Rac/Rop-Rboh signaling module mediates a basal ROS level in mature stigmas before pollination and controls changes in the stigmatic ROS status elicited by SI and CP (Figures 7I and 7J). Involvement of FER-regulated ROS has been well established during different steps of plant reproduction.  $^{25,27,28,34,67,68}$  FER regulates the accumulation of ovular ROS to support pollen tube rupture and sperm release for fertilization. 28,67,68 Its male counterparts, ANX1 and ANX2, act redundantly to maintain ROS in pollen to ensure pollen tube integrity.<sup>27</sup> As shown here and in Liu et al., 70 FER is crucial for maintaining Arabidopsis stigmatic ROS, which is suppressed upon pollination to promote pollen tube growth (Figure 7A). The determination of how ROS underlie SI and CP responses on the stigma here reveals another important functional role for these ubiquitous signaling intermediates. Elucidating the linkage between stigmatic ROS status and FER-Rac/Rop-Rboh signaling provides mechanistic insight into a pollen-stigma interactive process crucial for pollen acceptance or rejection on the receptive surface of the pistil (Figures 7I and 7J).

Although it is clear that activating ROS production is crucial for the SI response, how self-pollen recognition triggers the FER-Rac/Rop-regulated process remains to be investigated. Nevertheless, stigmatic ROS are developmentally regulated in ornamental kale<sup>38</sup> and in Chinese cabbage (Figure S2K), similar to the typical increase of SRK expression and SI strength from bud to mature stage stigmas in Brassica flowers.<sup>21</sup> Together with S-haplotype-specific increase of stigmatic ROS after selfpollination (Figure 2), these observations strongly suggest that the SP11/SCR-stimulated signaling interacts with and activates the FER-Rac/Rop-Rbohs module to generate high levels of ROS to reject self-pollen (Figure 7J). It would be interesting to investigate whether SRK or MLPK might phosphorylate and activate FER, thereby conferring S-haplotype-specific regulation of FER-Rac/ROP-Rbohs during SI responses (Figure 7J). Pollen grains secrete a large number of pollen coat proteins (PCPs),<sup>72</sup> which might be recognized specifically by their cognate receptors from the stigma to mediate germination of compatible pollen, such as the PCP-B class peptides in Arabidopsis. 70,71 The fact that the FER-Rac/Rop-Rboh module is also responsible for maintaining the basal stigmatic ROS levels and downregulated upon CP to promote compatible-pollen growth (Figure 7I)<sup>70</sup> is consistent with the signaling pathway being highly versatile, thus conserved to support CP and block SI pollination.

To establish how ROS impact various cellular events to regulate specific biological processes has remained challenging, largely due to their complex activities and the broad range of their target molecules. The utilization of NADPH-oxidase-dependent ROS to reject self-pollen on the stigma could be grounded on their toxic effects. 31,51,73-75 As NADPH oxidases produce superoxide in the apoplast of stigmatic papilla cells, high levels of ROS at the contact site of a self-pollen grain could immediately cause its arrest. Interestingly, although SI-induced ROS did not cause cell death in stigmatic papilla cells, compatible-pollinated stigmas in Brassica species rapidly initiate cell death. 47,48,76 Therefore, self-pollen arrest is not a result of the pollen grain just simply succumbing to an overwhelming injury caused by SI-induced ROS. Instead, given the intimate connection between ROS and many cellular events associated with pollen growth, such as Ca<sup>2+</sup> homeostasis, <sup>27,28,77</sup> actin organization, <sup>78</sup> or cell wall restructuring, <sup>27,79</sup> high levels of stigmatic ROS could inhibit these key processes during the SI response. Alternatively, the actin cytoskeleton could be prevented by the elevated stigmatic ROS from focalizing at the contact site with the pollen,79-82 thus prohibiting the delivery of secretory vesicles to support pollen growth.15

CP-induced decline together with self-pollen-triggered increase in stigmatic ROS being conserved in sporophytic SI systems (Figures 1, 2, and 5) suggest that the functional versatility of ROS must be well suited as a mediator of varied pollen responses, perhaps acting as a rheostat to fine-tune events that underlie SI or CP responses. Remarkably, the self-polleninduced increase and compatible-pollen-induced decline of stigmatic ROS are both locally restricted (Figures 3E, S3H, and S3I), thus ensuring selective arrest of self-pollen without interfering with compatible pollen tube development in the vicinity. The inhibitory effect of ROS in unpollinated stigmas on compatible pollen growth (Figures 4F, 4G, 6I, 7B, and 7F) and the accumulation of higher levels of ROS in mature stigmas than bud stage stigmas 35-38 (Figure S2K) are consistent with ROS fostering a defense function against pathogen attack before pollination. 35-38 However, the role of ROS on pollen-stigma interactions has been ambiguous,38 largely due to high concentrations of ROS inhibitors impeding the growth of both compatible and SI pollen (Figure S4A). However, at sub-inhibitory levels, such as 2 mM DPI, they effectively broke down SI (Figures 4A, 4B, S4A, and S4B), similar to kaempferol, another ROS scavenger, treatment of ornamental kale stigmas.38 Results from combined pharmaceutical and genetic suppression studies here therefore unequivocally establish ROS as crucial for the SI Please cite this article in press as: Zhang et al., FERONIA receptor kinase-regulated reactive oxygen species mediate self-incompatibility in *Brassica rapa*, Current Biology (2021), https://doi.org/10.1016/j.cub.2021.04.060





response, providing the foundation for further research on how stigmatic ROS are regulated during SI response for self-pollen rejection.

ROS also participate in other extensively studied SI systems, the PCD-based SI in *Papaveraceae*<sup>78,83–85</sup> and the S-RNase-based SI in *Pyrus pyrifolia*, <sup>86,87</sup> where stylar signals trigger inhibition of self-pollen tubes. Although these and the Brassicacea systems differ from one another, <sup>5,6,84,86,88</sup> the remarkable coincidence of ROS being a central component of their respective SI response suggests that SI-induced ROS increase in the signal-receptive side of the interaction might be a common event leading to self-pollen rejection.

#### **STAR**\*METHODS

Detailed methods are provided in the online version of this paper and include the following:

- KEY RESOURCES TABLE
- RESOURCE AVAILABILITY
  - Lead contact
  - Materials availability
  - Data and code availability
- EXPERIMENTAL MODEL AND SUBJECT DETAILS
- METHOD DETAILS
  - Excised stigma-feeding assays and pollen tube visualization
  - ODN design and treatment
  - Stigmatic ROS detection
  - NADPH-oxidase activity test
  - RNA isolation, cDNA synthesis and quantitative RTqPCR
  - O Molecular cloning and infiltration with Agrobacteria
  - Recombinant Protein expression and Purification, pull down assay
- QUANTIFICATION AND STATISTICAL ANALYSIS

#### SUPPLEMENTAL INFORMATION

Supplemental information can be found online at https://doi.org/10.1016/j.cub.2021.04.060.

#### **ACKNOWLEDGMENTS**

We thank Shunong Bai (Peking University) and Yujin Hao (Shandong Agriculture University) for discussions during various stages of this project. This work was supported in part by Research Start-up Fund from Shandong Agriculture University, the Key Program of Shandong Province Science Foundation (ZR2020KC017), US-NSF-1147165, and UMass NIFA/USDA MAS00525. The author ORCIDs are as follows: Q.D. 0000-0001-9016-8904; J. Huang 0000-0002-5960-9414; A.Y.C. 0000-0002-7973-022X; and H.-M.W. 0000-0003-2108-3848.

#### **AUTHOR CONTRIBUTIONS**

Q.D. conceptualized and designed the research plan and led the writing process. Q.D., J. Huang, and Y.Y. designed the experiments with contribution from X.W. L.Z. and J. Huang performed all experiments and data analysis with help from H.Z., J.Y., J.W., J. Hui, S.H., S. Song, Y.C., and M.W.; S. Su performed ODN-related experiments; L.Y. performed *Arabidopsis*-mutant-related experiments; and X.W. generated Chinese cabbage germplasm resources and performed S-haplotype-related experiments with help from Xiaowei Zhang,

Y.Z., and Z.W. W.Z. participated in data analysis and manuscript writing. Xiansheng Zhang contributed to project discussion and advanced the project. A.Y.C. and H.-M.W. contributed to project conceptualization, result interpretation, and manuscript writing. All participated in finalizing the manuscript.

#### **DECLARATION OF INTERESTS**

The authors declare no competing interests.

Received: April 23, 2020 Revised: January 18, 2021 Accepted: April 26, 2021 Published: May 19, 2021

#### **REFERENCES**

- Takayama, S., Shimosato, H., Shiba, H., Funato, M., Che, F.S., Watanabe, M., Iwano, M., and Isogai, A. (2001). Direct ligand-receptor complex interaction controls Brassica self-incompatibility. Nature 413, 534–538
- Kachroo, A., Schopfer, C.R., Nasrallah, M.E., and Nasrallah, J.B. (2001).
   Allele-specific receptor-ligand interactions in Brassica self-incompatibility. Science 293, 1824–1826.
- Shimosato, H., Yokota, N., Shiba, H., Iwano, M., Entani, T., Che, F.S., Watanabe, M., Isogai, A., and Takayama, S. (2007). Characterization of the SP11/SCR high-affinity binding site involved in self/nonself recognition in brassica self-incompatibility. Plant Cell 19, 107–117.
- Ma, R., Han, Z., Hu, Z., Lin, G., Gong, X., Zhang, H., Nasrallah, J.B., and Chai, J. (2016). Structural basis for specific self-incompatibility response in Brassica. Cell Res. 26, 1320–1329.
- Nasrallah, J.B. (2019). Self-incompatibility in the Brassicaceae: regulation and mechanism of self-recognition. Curr. Top. Dev. Biol. 131, 435–452
- Jany, E., Nelles, H., and Goring, D.R. (2019). The molecular and cellular regulation of Brassicaceae self-incompatibility and self-pollen rejection. Int. Rev. Cell Mol. Biol. 343, 1–35.
- Murase, K., Shiba, H., Iwano, M., Che, F.S., Watanabe, M., Isogai, A., and Takayama, S. (2004). A membrane-anchored protein kinase involved in Brassica self-incompatibility signaling. Science 303, 1516–1519.
- Gu, T., Mazzurco, M., Sulaman, W., Matias, D.D., and Goring, D.R. (1998). Binding of an arm repeat protein to the kinase domain of the S-locus receptor kinase. Proc. Natl. Acad. Sci. USA 95, 382–387.
- Kakita, M., Murase, K., Iwano, M., Matsumoto, T., Watanabe, M., Shiba, H., Isogai, A., and Takayama, S. (2007). Two distinct forms of M-locus protein kinase localize to the plasma membrane and interact directly with S-locus receptor kinase to transduce self-incompatibility signaling in Brassica rapa. Plant Cell 19, 3961–3973.
- Kitashiba, H., Liu, P., Nishio, T., Nasrallah, J.B., and Nasrallah, M.E. (2011). Functional test of Brassica self-incompatibility modifiers in Arabidopsis thaliana. Proc. Natl. Acad. Sci. USA 108, 18173–18178.
- Gao, Q., Shi, S., Liu, Y., Pu, Q., Liu, X., Zhang, Y., and Zhu, L. (2016). Identification of a novel MLPK homologous gene MLPKn1 and its expression analysis in Brassica oleracea. Plant Reprod. 29, 239–250.
- Chen, F., Yang, Y., Li, B., Liu, Z., Khan, F., Zhang, T., Zhou, G., Tu, J., Shen, J., Yi, B., et al. (2019). Functional analysis of M-locus protein kinase revealed a novel regulatory mechanism of self-incompatibility in *Brassica* napus L. Int. J. Mol. Sci. 20, 3303.
- Stone, S.L., Arnoldo, M., and Goring, D.R. (1999). A breakdown of Brassica self-incompatibility in ARC1 antisense transgenic plants. Science 286, 1729–1731.
- Stone, S.L., Anderson, E.M., Mullen, R.T., and Goring, D.R. (2003). ARC1 is an E3 ubiquitin ligase and promotes the ubiquitination of proteins during the rejection of self-incompatible Brassica pollen. Plant Cell 15, 885–898.

#### **Article**



- Samuel, M.A., Chong, Y.T., Haasen, K.E., Aldea-Brydges, M.G., Stone, S.L., and Goring, D.R. (2009). Cellular pathways regulating responses to compatible and self-incompatible pollen in Brassica and Arabidopsis stigmas intersect at Exo70A1, a putative component of the exocyst complex. Plant Cell 21, 2655–2671.
- Sankaranarayanan, S., Jamshed, M., and Samuel, M.A. (2015).
   Degradation of glyoxalase I in Brassica napus stigma leads to self-incompatibility response. Nat. Plants 1, 15185.
- Liu, J., Zhang, H., Lian, X., Converse, R., and Zhu, L. (2016). Identification
  of interacting motifs between Armadillo repeat containing 1 (ARC1) and
  Exocyst 70 A1 (Exo70A1) proteins in Brassica oleracea. Protein J. 35,
  34–43.
- Scandola, S., and Samuel, M.A. (2019). A flower-specific phospholipase D is a stigmatic compatibility factor targeted by the self-incompatibility response in Brassica napus. Curr. Biol. 29, 506–512.e4.
- Indriolo, E., Tharmapalan, P., Wright, S.I., and Goring, D.R. (2012). The ARC1 E3 ligase gene is frequently deleted in self-compatible Brassicaceae species and has a conserved role in Arabidopsis lyrata self-pollen rejection. Plant Cell 24, 4607–4620.
- Indriolo, E., Safavian, D., and Goring, D.R. (2014). The ARC1 E3 ligase promotes two different self-pollen avoidance traits in Arabidopsis. Plant Cell 26, 1525–1543.
- Nasrallah, M.E., Liu, P., and Nasrallah, J.B. (2002). Generation of self-incompatible Arabidopsis thaliana by transfer of two S locus genes from A. Iyrata. Science 297, 247–249.
- Nasrallah, J.B., and Nasrallah, M.E. (2014). Robust self-incompatibility in the absence of a functional ARC1 gene in Arabidopsis thaliana. Plant Cell 26, 3838–3841.
- Goring, D.R., Indriolo, E., and Samuel, M.A. (2014). The ARC1 E3 ligase promotes a strong and stable self-incompatibility response in Arabidopsis species: response to the Nasrallah and Nasrallah commentary. Plant Cell 26, 3842–3846.
- 24. Zhang, T., Zhou, G., Goring, D.R., Liang, X., Macgregor, S., Dai, C., Wen, J., Yi, B., Shen, J., Tu, J., et al. (2019). Generation of transgenic self-incompatible *Arabidopsis thaliana* shows a genus-specific preference for self-incompatibility genes. Plants 8, 570.
- 25. Potocký, M., Jones, M.A., Bezvoda, R., Smirnoff, N., and Žárský, V. (2007). Reactive oxygen species produced by NADPH oxidase are involved in pollen tube growth. New Phytol. 174, 742–751.
- Duan, Q., Kita, D., Li, C., Cheung, A.Y., and Wu, H.M. (2010). FERONIA receptor-like kinase regulates RHO GTPase signaling of root hair development. Proc. Natl. Acad. Sci. USA 107, 17821–17826.
- Boisson-Dernier, A., Lituiev, D.S., Nestorova, A., Franck, C.M., Thirugnanarajah, S., and Grossniklaus, U. (2013). ANXUR receptor-like kinases coordinate cell wall integrity with growth at the pollen tube tip via NADPH oxidases. PLoS Biol. 11, e1001719.
- Duan, Q., Kita, D., Johnson, E.A., Aggarwal, M., Gates, L., Wu, H.M., and Cheung, A.Y. (2014). Reactive oxygen species mediate pollen tube rupture to release sperm for fertilization in Arabidopsis. Nat. Commun. 5, 3129.
- Xie, H.T., Wan, Z.Y., Li, S., and Zhang, Y. (2014). Spatiotemporal production of reactive oxygen species by NADPH oxidase is critical for tapetal programmed cell death and pollen development in Arabidopsis. Plant Cell 26, 2007–2023.
- Yu, S.X., Feng, Q.N., Xie, H.T., Li, S., and Zhang, Y. (2017). Reactive oxygen species mediate tapetal programmed cell death in tobacco and tomato. BMC Plant Biol. 17, 76.
- 31. Mittler, R. (2017). ROS are good. Trends Plant Sci. 22, 11-19.
- 32. Li, Q., Ai, G., Shen, D., Zou, F., Wang, J., Bai, T., Chen, Y., Li, S., Zhang, M., Jing, M., and Dou, D. (2019). A Phytophthora capsici effector targets ACD11 binding partners that regulate ROS-mediated defense response in Arabidopsis. Mol. Plant 12, 565–581.

- Zhang, M.J., Zhang, X.S., and Gao, X.Q. (2020). ROS in the male-female interactions during pollination: function and regulation. Front. Plant Sci. 11, 177.
- 34. Feng, H., Liu, C., Fu, R., Zhang, M., Li, H., Shen, L., Wei, Q., Sun, X., Xu, L., Ni, B., and Li, C. (2019). LORELEI-LIKE GPI-ANCHORED PROTEINS 2/3 regulate pollen tube growth as chaperones and coreceptors for ANXUR/BUPS receptor kinases in Arabidopsis. Mol. Plant 12, 1612–1623.
- McInnis, S.M., Desikan, R., Hancock, J.T., and Hiscock, S.J. (2006).
   Production of reactive oxygen species and reactive nitrogen species by angiosperm stigmas and pollen: potential signalling crosstalk? New Phytol. 172, 221–228.
- McInnis, S.M., Emery, D.C., Porter, R., Desikan, R., Hancock, J.T., and Hiscock, S.J. (2006). The role of stigma peroxidases in flowering plants: insights from further characterization of a stigma-specific peroxidase (SSP) from Senecio squalidus (Asteraceae). J. Exp. Bot. 57, 1835–1846.
- Zafra, A., Rejón, J.D., Hiscock, S.J., and Alché, Jde.D. (2016). Patterns of ROS accumulation in the stigmas of angiosperms and visions into their multi-functionality in plant reproduction. Front. Plant Sci. 7, 1112.
- Lan, X., Yang, J., Abhinandan, K., Nie, Y., Li, X., Li, Y., and Samuel, M.A. (2017). Flavonoids and ROS play opposing roles in mediating pollination in ornamental kale (Brassica oleracea var. acephala). Mol. Plant 10, 1361–1364.
- Nou, S., Watanabe, M., Isogai, A., and Hinata, K. (1993). Comparison of S-alleles and S-glycoproteins between two wild population of *Brassica* campestris in Turkey and Japan. Sex. Plant Reprod. 6, 79–86.
- Bright, J., Desikan, R., Hancock, J.T., Weir, I.S., and Neill, S.J. (2006).
   ABA-induced NO generation and stomatal closure in Arabidopsis are dependent on H2O2 synthesis. Plant J. 45, 113–122.
- 41. Zeng, L., Zhou, J., Li, B., and Xing, D. (2015). A high-sensitivity optical device for the early monitoring of plant pathogen attack via the in vivo detection of ROS bursts. Front. Plant Sci. 6, 96.
- Liao, F., Wang, L., Yang, L.-B., Zhang, L., Peng, X., and Sun, M.X. (2013).
   Antisense oligodeoxynucleotide inhibition as an alternative and convenient method for gene function analysis in pollen tubes. PLoS ONE 8, e59112.
- Bezvoda, R., Pleskot, R., Zárský, V., and Potocký, M. (2014). Antisense oligodeoxynucleotide-mediated gene knockdown in pollen tubes. Methods Mol. Biol. 1080, 231–236.
- Mizuta, Y., and Higashiyama, T. (2014). Antisense gene inhibition by phosphorothioate antisense oligonucleotide in Arabidopsis pollen tubes. Plant J. 78, 516–526.
- Chai, L., Tudor, R.L., Poulter, N.S., Wilkins, K.A., Eaves, D.J., Franklin, F.C.H., and Franklin-Tong, V.E. (2017). MAP kinase PrMPK9-1 contributes to the self-incompatibility response. Plant Physiol. 174, 1226–1237.
- Chen, J., Wang, P., de Graaf, B.H.J., Zhang, H., Jiao, H., Tang, C., Zhang, S., and Wu, J. (2018). Phosphatidic acid counteracts S-RNase signaling in pollen by stabilizing the actin cytoskeleton. Plant Cell 30, 1023–1039.
- Su, S., Dai, H., Wang, X., Wang, C., Zeng, W., Huang, J., and Duan, Q. (2020). Ethylene negatively mediates self-incompatibility response in Brassica rapa. Biochem. Biophys. Res. Commun. 525, 600–606.
- 48. Huang, J., Su, S., Dai, H., Liu, C., Wei, X., Zhao, Y., Wang, Z., Zhang, X., Yuan, Y., Yu, X., et al. (2020). Programmed cell death in stigmatic papilla cells is associated with senescence-induced self-incompatibility breakdown in Chinese cabbage and radish. Front. Plant Sci. 11, 586901.
- 49. Qi, J., Wang, J., Gong, Z., and Zhou, J.M. (2017). Apoplastic ROS signaling in plant immunity. Curr. Opin. Plant Biol. 38, 92–100.
- Shetty, N.P., Kristensen, B.K., Newman, M.-A., Møller, K., Gregersen, P.L., and Jørgensen, H.J.L. (2003). Association of hydrogen peroxide with restriction of *Septoria tritici* in resistant wheat. Physiol. Mol. Plant Pathol. 62, 333–346.
- Miller, E.W., Dickinson, B.C., and Chang, C.J. (2010). Aquaporin-3 mediates hydrogen peroxide uptake to regulate downstream intracellular signaling. Proc. Natl. Acad. Sci. USA 107, 15681–15686.

Please cite this article in press as: Zhang et al., FERONIA receptor kinase-regulated reactive oxygen species mediate self-incompatibility in *Brassica rapa*, Current Biology (2021), https://doi.org/10.1016/j.cub.2021.04.060



# Current Biology

- Nathan, C., and Cunningham-Bussel, A. (2013). Beyond oxidative stress: an immunologist's guide to reactive oxygen species. Nat. Rev. Immunol. 13, 349–361.
- 53. Gilroy, S., Suzuki, N., Miller, G., Choi, W.G., Toyota, M., Devireddy, A.R., and Mittler, R. (2014). A tidal wave of signals: calcium and ROS at the forefront of rapid systemic signaling. Trends Plant Sci. 19, 623–630.
- 54. Otulak-Kozieł, K., Kozieł, E., Bujarski, J.J., Frankowska-Łukawska, J., and Torres, M.A. (2020). Respiratory burst oxidase homologs RBOHD and RBOHF as key modulating components of response in turnip mosaic virus-Arabidopsisthaliana (L.) Heyhn system. Int. J. Mol. Sci. 21, 8510.
- Torres, M.A., Jones, J.D.G., and Dangl, J.L. (2005). Pathogen-induced, NADPH oxidase-derived reactive oxygen intermediates suppress spread of cell death in Arabidopsis thaliana. Nat. Genet. 37, 1130–1134.
- Cheng, F., Liu, S., Wu, J., Fang, L., Sun, S., Liu, B., Li, P., Hua, W., and Wang, X. (2011). BRAD, the genetics and genomics database for Brassica plants. BMC Plant Biol. 11, 136.
- Wang, X., Wu, J., Liang, J., Cheng, F., and Wang, X. (2015). Brassica database (BRAD) version 2.0: integrating and mining Brassicaceae species genomic resources. Database (Oxford) 2015, bav093.
- Cai, C., Wang, X., Liu, B., Wu, J., Liang, J., Cui, Y., Cheng, F., and Wang, X. (2017). Brassica rapa Genome 2.0: a reference upgrade through sequence re-assembly and gene re-annotation. Mol. Plant 10, 649–651.
- Bechsgaard, J.S., Castric, V., Charlesworth, D., Vekemans, X., and Schierup, M.H. (2006). The transition to self-compatibility in Arabidopsis thaliana and evolution within S-haplotypes over 10 Myr. Mol. Biol. Evol. 23, 1741–1750.
- Boggs, N.A., Nasrallah, J.B., and Nasrallah, M.E. (2009). Independent Slocus mutations caused self-fertility in Arabidopsis thaliana. PLoS Genet. 5. e1000426.
- 61. Suwabe, K., Nagasaka, K., Windari, E.A., Hoshiai, C., Ota, T., Takada, M., Kitazumi, A., Masuko-Suzuki, H., Kagaya, Y., Yano, K., et al. (2020). Double-locking mechanism of self-compatibility in *Arabidopsis thaliana*: the synergistic effect of transcriptional depression and disruption of coding region in the male specificity gene. Front. Plant Sci. 11, 576140.
- 62. Alonso, J.M., Stepanova, A.N., Leisse, T.J., Kim, C.J., Chen, H., Shinn, P., Stevenson, D.K., Zimmerman, J., Barajas, P., Cheuk, R., et al. (2003). Genome-wide insertional mutagenesis of Arabidopsis thaliana. Science 301, 653–657.
- Nibau, C., Wu, H.M., and Cheung, A.Y. (2006). RAC/ROP GTPases: 'hubs' for signal integration and diversification in plants. Trends Plant Sci. 11, 309–315
- 64. Wong, H.L., Pinontoan, R., Hayashi, K., Tabata, R., Yaeno, T., Hasegawa, K., Kojima, C., Yoshioka, H., Iba, K., Kawasaki, T., and Shimamoto, K. (2007). Regulation of rice NADPH oxidase by binding of Rac GTPase to its N-terminal extension. Plant Cell 19, 4022–4034.
- 65. Kosami, K., Ohki, I., Nagano, M., Furuita, K., Sugiki, T., Kawano, Y., Kawasaki, T., Fujiwara, T., Nakagawa, A., Shimamoto, K., and Kojima, C. (2014). The crystal structure of the plant small GTPase OsRac1 reveals its mode of binding to NADPH oxidase. J. Biol. Chem. 289, 28569–28578.
- Qu, Y., Yan, M., and Zhang, Q. (2017). Functional regulation of plant NADPH oxidase and its role in signaling. Plant Signal. Behav. 12, e1356970.
- 67. Li, C., Yeh, F.L., Cheung, A.Y., Duan, Q., Kita, D., Liu, M.C., Maman, J., Luu, E.J., Wu, B.W., Gates, L., et al. (2015). Glycosylphosphatidylinositol-anchored proteins as chaperones and co-receptors for FERONIA receptor kinase signaling in Arabidopsis. eLife 4, e06587.
- 68. Escobar-Restrepo, J.M., Huck, N., Kessler, S., Gagliardini, V., Gheyselinck, J., Yang, W.C., and Grossniklaus, U. (2007). The FERONIA receptor-like kinase mediates male-female interactions during pollen tube reception. Science 317, 656–660.
- Rotman, N., Rozier, F., Boavida, L., Dumas, C., Berger, F., and Faure, J.E. (2003). Female control of male gamete delivery during fertilization in Arabidopsis thaliana. Curr. Biol. 13, 432–436.

- Liu, C., Shen, L., Xiao, Y., Vyshedsky, D., Peng, C., Sun, X., Liu, Z., Cheng, L., Zhang, H., Han, Z., et al. (2021). Pollen PCP-B peptides unlock a stigma peptide-receptor kinase gating mechanism for pollination. Science 372, 171–175.
- Wang, L., Clarke, L.A., Eason, R.J., Parker, C.C., Qi, B., Scott, R.J., and Doughty, J. (2017). PCP-B class pollen coat proteins are key regulators of the hydration checkpoint in Arabidopsis thaliana pollen-stigma interactions. New Phytol. 213, 764–777.
- Doughty, J., Hedderson, F., McCubbin, A., and Dickinson, H. (1993). Interaction between a coating-borne peptide of the Brassica pollen grain and stigmatic S (self-incompatibility)-locus-specific glycoproteins. Proc. Natl. Acad. Sci. USA 90, 467–471.
- Lamb, C., and Dixon, R.A. (1997). The oxidative burst in plant disease resistance. Annu. Rev. Plant Physiol. Plant Mol. Biol. 48, 251–275.
- Møller, I.M., Jensen, P.E., and Hansson, A. (2007). Oxidative modifications to cellular components in plants. Annu. Rev. Plant Biol. 58, 459–481.
- Camejo, D., Guzmán-Cedeño, Á., and Moreno, A. (2016). Reactive oxygen species, essential molecules, during plant-pathogen interactions. Plant Physiol. Biochem. 103, 10–23.
- 76. Sankaranarayanan, S., Jamshed, M., Deb, S., Chatfield-Reed, K., Kwon, E.-J.G., Chua, G., and Samuel, M.A. (2013). Deciphering the stigmatic transcriptional landscape of compatible and self-incompatible pollinations in Brassica napus reveals a rapid stigma senescence response following compatible pollination. Mol. Plant 6, 1988–1991.
- 77. Wu, J., Shang, Z., Wu, J., Jiang, X., Moschou, P.N., Sun, W., Roubelakis-Angelakis, K.A., and Zhang, S. (2010). Spermidine oxidase-derived H<sub>2</sub>O<sub>2</sub> regulates pollen plasma membrane hyperpolarization-activated Ca(2+) -permeable channels and pollen tube growth. Plant J. 63, 1042–1053.
- Wilkins, K.A., Bancroft, J., Bosch, M., Ings, J., Smirnoff, N., and Franklin-Tong, V.E. (2011). Reactive oxygen species and nitric oxide mediate actin reorganization and programmed cell death in the self-incompatibility response of papaver. Plant Physiol. 156, 404–416.
- Mangano, S., Juárez, S.P., and Estevez, J.M. (2016). ROS regulation of polar growth in plant cells. Plant Physiol. 171, 1593–1605.
- 80. Iwano, M., Shiba, H., Matoba, K., Miwa, T., Funato, M., Entani, T., Nakayama, P., Shimosato, H., Takaoka, A., Isogai, A., and Takayama, S. (2007). Actin dynamics in papilla cells of Brassica rapa during self-and cross-pollination. Plant Physiol. 144, 72–81.
- Rozier, F., Riglet, L., Kodera, C., Bayle, V., Durand, E., Schnabel, J., Gaude, T., and Fobis-Loisy, I. (2020). Live-cell imaging of early events following pollen perception in self-incompatible Arabidopsis thaliana. J. Exp. Bot. 71, 2513–2526.
- Bosch, M., and Wang, L. (2020). Pollen-stigma interactions in Brassicaceae: complex communication events regulating pollen hydration. J. Exp. Bot. 71, 2465–2468.
- Bosch, M., Poulter, N.S., Vatovec, S., and Franklin-Tong, V.E. (2008). Initiation of programmed cell death in self-incompatibility: role for cyto-skeleton modifications and several caspase-like activities. Mol. Plant 1, 879–887
- 84. Wilkins, K.A., Poulter, N.S., and Franklin-Tong, V.E. (2014). Taking one for the team: self-recognition and cell suicide in pollen. J. Exp. Bot. 65, 1331–1342.
- Eaves, D.J., Flores-Ortiz, C., Haque, T., Lin, Z., Teng, N., and Franklin-Tong, V.E. (2014). Self-incompatibility in Papaver: advances in integrating the signalling network. Biochem. Soc. Trans. 42, 370–376.
- 86. Wang, C.L., Wu, J., Xu, G.H., Gao, Y.B., Chen, G., Wu, J.Y., Wu, H.Q., and Zhang, S.L. (2010). S-RNase disrupts tip-localized reactive oxygen species and induces nuclear DNA degradation in incompatible pollen tubes of Pyrus pyrifolia. J. Cell Sci. 123, 4301–4309.
- 87. Jiang, X., Gao, Y., Zhou, H., Chen, J., Wu, J., and Zhang, S. (2014). Apoplastic calmodulin promotes self-incompatibility pollen tube growth by enhancing calcium influx and reactive oxygen species concentration in Pyrus pyrifolia. Plant Cell Rep. 33, 255–263.

Please cite this article in press as: Zhang et al., FERONIA receptor kinase-regulated reactive oxygen species mediate self-incompatibility in Brassica rapa, Current Biology (2021), https://doi.org/10.1016/j.cub.2021.04.060

## **Current Biology**

#### **Article**



- 88. Bedinger, P.A., Broz, A.K., Tovar-Mendez, A., and McClure, B. (2017). Pollen-pistil interactions and their role in mate selection. Plant Physiol.
- 89. Shen, W.J., and Forde, B.G. (1989). Efficient transformation of Agrobacterium spp. by high voltage electroporation. Nucleic Acids Res 17 8385
- 90. Tissier, A.F., Marillonnet, S., Klimyuk, V., Patel, K., Torres, M.A., Murphy, G., and Jones, J.D. (1999). Multiple independent defective suppressormutator transposon insertions in Arabidopsis: a tool for functional genomics. Plant Cell 11, 1841-1852.
- 91. Huang, J.B., Liu, H., Chen, M., Li, X., Wang, M., Yang, Y., Wang, C., Huang, J., Liu, G., Liu, Y., et al. (2014). ROP3 GTPase contributes to polar auxin transport and auxin responses and is important for embryogenesis and seedling growth in Arabidopsis. Plant Cell 26, 3501-3518.
- 92. Rueden, C.T., Schindelin, J., Hiner, M.C., DeZonia, B.E., Walter, A.E., Arena, E.T., and Eliceiri, K.W. (2017). ImageJ2: ImageJ for the next generation of scientific image data. BMC Bioinformatics 18, 529.
- 93. Smyth, D.R., Bowman, J.L., and Meyerowitz, E.M. (1990). Early flower development in Arabidopsis. Plant Cell 2, 755-767.
- 94. Duan, Q., Liu, M.J., Kita, D., Jordan, S.S., Yeh, F.J., Yvon, R., Carpenter, H., Federico, A.N., Garcia-Valencia, L.E., Eyles, S.J., et al. (2020).

- FERONIA controls pectin- and nitric oxide-mediated male-female interaction. Nature 579, 561-566.
- 95. Henry, E., Fung, N., Liu, J., Drakakaki, G., and Coaker, G. (2015). Beyond glycolysis: GAPDHs are multi-functional enzymes involved in regulation of ROS, autophagy, and plant immune responses. PLoS Genet. 11, e1005199.
- 96. Rutley, N., and Miller, G. (2020). Large-scale analysis of pollen viability and oxidative level using H<sub>2</sub>DCFDA-staining coupled with flow cytometry. Methods Mol. Biol. 2160, 167-179.
- 97. Dunand, C., Crèvecoeur, M., and Penel, C. (2007). Distribution of superoxide and hydrogen peroxide in Arabidopsis root and their influence on root development: possible interaction with peroxidases. New Phytol.
- 98. Sandalio, L.M., Rodríguez-Serrano, M., Romero-Puertas, M.C., and Del Río, L.A. (2008). Imaging of reactive oxygen species and nitric oxide in vivo in plant tissues. Methods Enzymol. 440, 397-409.
- 99. Hajdukiewicz, P., Svab, Z., and Maliga, P. (1994). The small, versatile pPZP family of Agrobacterium binary vectors for plant transformation. Plant Mol. Biol. 25, 989-994.
- 100. Louvet, O., Doignon, F., and Crouzet, M. (1997). Stable DNA-binding yeast vector allowing high-bait expression for use in the two-hybrid system. Biotechniques 23, 816-818, 820.





#### **STAR**\***METHODS**

#### **KEY RESOURCES TABLE**

REAGENT or RESOURCE	SOURCE	IDENTIFIER
Antibodies		
Anti-Myc	Abmart	M20002; RRID: AB_2861172
Anti-GST	Abmart	M20007; RRID: AB_2864360
Anti-His	Abmart	M30111; RRID: AB_2889874
Goat Anti-Mouse	Abmart	M21001; RRID: AB_2713950
Bacterial and virus strains		
Agrobacterium tumefaciens LBA4404	TransGen Biotech <sup>89</sup>	N/A
E. coli DH5α (Trans-T1)	TransGen Biotech	CD501-01
E. coli BL21 (DE3)	TransGen Biotech	CD601-02
Chemicals, peptides, and recombinant proteins		
DPI	Sigma-Aldrich	43088
CuCl <sub>2</sub>	Sigma-Aldrich	222011
KI	KaiTong	GB/T 1272-200
Tiron	BBI Life Sciences	TB0951
Na-Benzoate	Sigma-Aldrich	B3420
Xanthine/Xanthine Oxidase	Sigma-Aldrich	X1875
FeSO <sub>4</sub>	Sigma-Aldrich	F8263
H₂DCFDA	Med Chem Express	HY-D0940
DHE	Yuanye Bio-Technology	S40454
HPF	Maokang Bio-Technology	MX4805
FM4-64	Maokang Bio-Technology	MX4016
Aniline Blue	Sigma-Aldrich	415049
oCAMBIA1300 BrRbohD1/D2/F/I	This study	N/A
oCXSN-56 BrFER1-N	This study	N/A
PGEX-4T-1 BrROP2	This study	N/A
PET-32a BrRbohF-N	This study	N/A
pGADT7 BrROP2	This study	N/A
pGBKT7 BrRbohF-N	This study	N/A
pGBKT7 BrRbohF-C	This study	N/A
Critical commercial assays		
GSH agarose beads	BEAVER	70601-100
TALON beads	Clontech	635606
Plant total protein extraction kit	Coolaber	PTE001-50T
NADPH-oxidase activity kit	mlbio	ml249150
RNAprep pure Micro Kit	TIANGEN	DP420
HiScript II1st Stand cDNA Synthesis Kit (+gDNA wiper)	Vazyme	R212-01/02
HiScript IIQ RT SuperMix for qPCR	Vazyme	R222-01
Hipure PCR Pure Mini Kit	Magen	D2121-03
oEASY-Basic Seamless Cloning and Assembly Kit	TransGen Biotech	CU201-03
TIANprep Mini Plasmid Kit	TIANGEN	DP103
Experimental models: organisms/strains		
A.thaliana: Col-0	Salk collection	N/A
A.thaliana: C24	Salk collection	N/A

(Continued on next page)

Please cite this article in press as: Zhang et al., FERONIA receptor kinase-regulated reactive oxygen species mediate self-incompatibility in Brassica rapa, Current Biology (2021), https://doi.org/10.1016/j.cub.2021.04.060

## **Current Biology**

#### **Article**



Continued		
REAGENT or RESOURCE	SOURCE	IDENTIFIER
A.thaliana: rbohD-3	Salk collection	Salk_070610C
A.thaliana: rbohD-4	Salk collection	CS9555
A.thaliana: fer-4	Salk collection	GK-106A06
A.thaliana: srn	Previous study <sup>69</sup>	N/A
A.thaliana: FER <sub>pro</sub> :FER-GFP	Previous study <sup>26</sup>	N/A
B.rapa: ZY15	This study	N/A
B.rapa: 14CR	This study	N/A
B.rapa: DHB 848	Seedland	N/A
B.rapa: R16	This study	N/A
Raphanus sativus: Weixianqing 40	This study	N/A
B. oleracea: Kamome red	Takii Seed	FHB571
Oligonucleotides		
Table S1 (Primers for <i>Arabidopsis</i> mutant confirmation)	This study	N/A
Primer for the border of atrbohD	Previous study <sup>90</sup>	N/A
Table S2 (Gene Accession numbers)	This study	N/A
Table S3 (S- or AS-ODNs)	This study	N/A
Table S4 (Primers for qRT-PCR)	This study	N/A
AtACTIN2 Primer for RT-PCR	Previous study <sup>91</sup>	N/A
Software and algorithms		
ImageJ	Rueden et al. <sup>92</sup> ; https://imagej.net/Welcome	J2
Prism	Alliance Development Group; https://www.graphpad-prism.cn/	V8.0

#### **RESOURCE AVAILABILITY**

#### **Lead contact**

Further information and request for resources and reagents should be directed to and will be fulfilled by the Lead Contact, Qiaohong Duan (duangh@sdau.edu.cn).

#### **Materials availability**

Plant materials and plasmids generated in this study will be made available on request, but we may require a payment and/or a completed Materials Transfer Agreement if there is potential for commercial application.

#### Data and code availability

This study did not generate any unique datasets or code.

#### **EXPERIMENTAL MODEL AND SUBJECT DETAILS**

Experiments performed with heading Chinese cabbage (Brassica rapa L. ssp. pekinensis) plants were mostly done using two selfincompatible cultivars, 14CR (a double haploid line with an S<sub>46</sub> haplotype) and ZY15 (a multi-generational inbred line with an S<sub>53</sub> haplotype) for self-pollination or cross-pollination. Two other Chinese cabbage cultivars, R16 (a double haploid line) and DHB848 (a commercial line), and two other Brassica species, radish (Raphanus sativus, a high-generation inbred line named "Weixianqing 40") and Ornamental kale (B. oleracea var. acephala, a commercial line named 'Kamome red") were used to verify the regulation of SI by stigmatic ROS. Seeds of Chinese cabbage, radish and ornamental kale were germinated in potted soil (Pindstrup substrate). Vernalization was performed in a growth chamber with 10°C/5°C, 14/10 h light/dark cycles, and light intensity of 100 μmol/m2/s. After 1 month of vernalization for 1 week-old Chinese cabbage and radish seedlings, and 3 months of vernalization for 7~8-leaf stage ornamental kale plants, these plants were planted in soil under greenhouse conditions with 25°C/15°C, 16/8 h light/dark cycles, and light intensity of 300 µmol/m2/s. The Arabidopsis thaliana T-DNA insertional mutants fer-4 (GK-106A06), AtrbohD-3 (Salk\_070610C), AtrbohD-4 (CS9555) are in Columbia ecotype; the  $\gamma$ -ray mutant sirene (srn)<sup>69</sup> is in C24 ecotype. Primer sequences for AtRbohD T-DNA mutant confirmation were listed in Table S1. Seeds of Arabidopsis and Nicotiana benthamiana were germinated and grew in potted soil in a green house.

Please cite this article in press as: Zhang et al., FERONIA receptor kinase-regulated reactive oxygen species mediate self-incompatibility in *Brassica rapa*, Current Biology (2021), https://doi.org/10.1016/j.cub.2021.04.060





#### **METHOD DETAILS**

#### Excised stigma-feeding assays and pollen tube visualization

Excised stigmas were treated as previously described  $^{47,48}$  in PGM (5 mM CaCl<sub>2</sub>, 5 mM KCl, 0.01% H<sub>3</sub>BO<sub>3</sub>, 1 mM MgSO<sub>4</sub>·7H<sub>2</sub>O, 10% sucrose, 0.8% agarose, pH7.5) or treatment medium (PGM supplemented with different concentrations of corresponding chemicals). Chemicals (Key resources table) used in the feeding assays include DPI, CuCl<sub>2</sub>, Tiron, KI, Na-Benzoate, Xanthine/Xanthine Oxidase, and FeSO<sub>4</sub>. Mock medium has the same amount of corresponding solvent.

Chinese cabbage flowers at stages analogous with *A. thaliana* stage 12 to stage 13 flowers, <sup>93</sup> i.e., they just start to open but before anther dehiscence, were emasculated. Stigmas were cut at 3 mm away from the stigmatic surface and inserted into basic PGM or the treatment medium and kept in a chamber with constant temperature (22.5°C) and humidity (45%). After 6 hours of treatment, stigmas were transferred to basic PGM medium and manually pollinated with similar amount of self– or cross–pollen grains so that each stigma was covered with only one layer of pollen grains. Stigmas were maintained in the same condition for 6 hours after pollination (HAP) then processed for aniline blue staining to visualize pollen tubes following the procedure as previously reported. <sup>94</sup> After pollination, stigmas were fixed in Canoy's fixative (methanol: acetic acid = 3:1), softened in 10 M NaOH, and stained in 0.1% aniline blue. Pollen tubes were visualized by epifluorescence (Ex375-328/DM415/BA351p) on a Nikon Eclipse Ni. Images were captured by a DS-Ri2 digital camera. The effect of chemicals on SI or on compatible pollinations were assessed by the number of pollen tubes that had penetrated the stigma papilla cells.

#### **ODN** design and treatment

Sense- and antisense-oligodeoxyribonucleotide (S-ODN and AS-ODN) were used to target the following genes (accession numbers shown in Table S2): BrRbohF, BrRbohD1, BrRbohD2, BrRbohI, BrRbohD2, and BrFER1. S- or AS-ODNs were designed based on Sfold (https://sfold.wadsworth.org/cgi-bin/soligo.pl). BLAST program (https://blast.ncbi.nlm.nih.gov/Blast.cgi) was used to assess potential off-target effect. The ODNs were synthesized in Beijing Genomics Institution (BGI). Three bases at both 5' and 3' end of S-ODN and AS-ODN were phosphorothioate-modified to maintain stability. The sequences of S-ODNs and AS-ODNs were listed in Table S3. ODN treatment of stigmas followed the methods of the stigma feeding assays<sup>47,48</sup> with some modifications. Stigmas of just open flowers were excised at the style 1 mm away from the top, inserted in PGM containing the S- or AS-ODN and treated for 1 hour. Two hours after pollination, stigmas were subjected to aniline blue assay for observation of pollen and pollen tube growth through microscopy.

#### **Stigmatic ROS detection**

Probe 2',7'-Dichlorodihydrofluorescein diacetate (H<sub>2</sub>DCFDA), dihydroethidium (DHE), hydroxyphenyl fluorescein (HPF) are commonly used for ROS detection.  $^{26,28,40,41,95-98}$  These three ROS probes (Key resources table) were used to get consistent conclusions about ROS status. If not specified, H<sub>2</sub>DCFDA was used for ROS staining. Protocol for stigmatic ROS staining using H<sub>2</sub>DCFDA followed that of ovular ROS staining.  $^{28}$  Stigmas were soaked in MES-KCI buffer (MES 10 mM, KCI 5  $\mu$ M, CaCl<sub>2</sub> 50  $\mu$ M, pH 6.15) for 30 min, stained with 50  $\mu$ M H<sub>2</sub>DCFDA for 1-2 hours, then washed at least 3 times before observation. This minimized signal variations due to dye accessibility issues. Staining conditions for DHE and HPF were similar as above described with the following modifications: DHE was used at 20  $\mu$ M in Tris-HCl buffer (10 mM Tris, pH 7.5) for 1 hour; HPF was used at 10  $\mu$ M in 0.2 M PBS buffer (pH 6.1) for 2 hours. Comparable results were obtained in experiments tested with all three dyes, providing confidence for the observed changes in ROS levels.

A Nikon Eclipse Ni and equipped with a DS-Ri2 digital camera was used for imaging.  $H_2DCFDA$  and HPF were observed under eGFP epifluorescence (Ex470-440, DM4951p, BA525/550). DHE were observed under eRFP epifluorescence (EX 560/540, DM590, BA5901p). If not specified, the exposure times for all comparative samples were exactly the same within one experiment. Between different experiments, exposure times were similar (e.g., between 800 ms to 900 ms under the 4x objective lens). ImageJ was used to quantify the average signal intensity in regions of interest (usually the whole stigma). Average ROS signals in control stigmas were set at 1 for comparative analyses.

#### **NADPH-oxidase activity test**

Stigmas were treated with the corresponding chemicals, S- or AS-ODNs, or pollination as indicated. For samples involving pollination, unpollinated or stigmas at 5, 10, 15 min after self- or cross-pollination were washed 6 times in 1.5 mL microfuge tubes with the MES-KCI buffer, i.e., the same buffer for stigma ROS staining, before frozen in liquid N<sub>2</sub>. NADPH-oxidase activity was measured following the instructions (mlbio). In brief, 0.05 g stigma tissue (~100 stigmas) was ground in liquid nitrogen, extracted in buffer (0.2 M NaH<sub>2</sub>PO4, 0.2 M Na<sub>2</sub>HPO4, pH7.2), and centrifuged at 3000 rpm for 20 min at 4°C. The crude extracts were used to measure NADPH-oxidase activity spectrophotometrically at 340 nm using FAD and NADPH as substrates.

#### RNA isolation, cDNA synthesis and quantitative RT-qPCR

Total RNA was extracted by the Plant total RNA extraction kit (TIANGEN, Beijing, China). Briefly, thirty stigmas were homogenized in 500  $\mu$ L lysis buffer with a RNase-free pestle in a microtube. The mix were vortexed for 30S, centrifuged at 12000 rpm for 10 min at 4°C. The supernatant was carefully transferred to a new centrifuge tube without disturbing the interphase and equal volume 70% ethanol was added into supernatant to precipitate the RNA. The RNA solution was then loaded onto an isolation column for RNA purification. The pellet was washed twice, followed by a DNase I (TAKARA) digest step to remove genomic DNA contamination. Finally,

Please cite this article in press as: Zhang et al., FERONIA receptor kinase-regulated reactive oxygen species mediate self-incompatibility in Brassica rapa, Current Biology (2021), https://doi.org/10.1016/j.cub.2021.04.060

# **Current Biology**

**Article** 



total RNA was eluted by RNase free ddH<sub>2</sub>O. The quality was assessed by 1% agarose gel electrophoresis and the quantification was performed using a Nanodrop 2000C (Thermo Scientific) spectrophotometer. cDNA synthesis was performed using a cDNA reverse transcript kit (Vazyme, Nanjing, China) according the manufactural instructions.

For RT-qPCR, the 20 μL reaction mixture was set up as follow: 2 × ChamQ SYBR qPCR Master Mix (Vazyme) 10 μL, cDNA 0.4 μL, gene specific primes 0.4 ul+0.4 ul, RNase free ddH<sub>2</sub>O 8.8 μL. The sequence of each primer used in this study was subjected to primer blast (NCBI) to ensure the specificity to the target gene. The specificity of the amplicons was further confirmed by the melt curves, which only showed a single peak. PCR was performed in a qTOWER<sup>3</sup> qPCR machine (Analytikjena, Germany) followed the parameter setting: 95°C for 30 s, 95°C for 10 s, 60°C for 22 s, 40 cycles. 2<sup>-ΔΔ</sup>Ct method was used to analyze the expression level of each gene. BrACTIN 2 or AtACTIN2 were used as the internal control.

#### Molecular cloning and infiltration with Agrobacteria

Full length CDS for BrRbohF, BrRbohD1, BrRbohD2, and BrRbohI were amplified with gene specific primers (Key resources table) using Phanta Max Super-Fidelity DNA Polymerase (Vazyme). PCR reaction included heat activation at 95°C for 3 min, denaturation at 95°C, for 15 s, annealing at 60°C for 15 s, extension at 72°C for 3 min and final extension at 72°C for 5 min, 35 cycles. After purification using the PCR product purification Kit (Magen), the DNA fragments were ligated to a GFP-fusion pCambia1300 vector. 99 The recombinant vector with the target DNA fragment was transformed into Agrobacterium tumefaciens LBA440489 via electric pulse-mediated method. For infiltration,<sup>67</sup> the agrobacteria cells were spin down at 4000 rpm for 10 min at 4°C. The pellet was resuspended to an OD<sub>600nm</sub> = 0.6 in infiltration buffer (10 mM MES, 10 mM MgCl<sub>2</sub>, 0.5% glucose, pH = 6.5). Before infiltration, acetosyringone was added to a final concentration of 100 μM. Leaves from 5-6 week-old tobacco plants (Nicotiana benthamiana) were infiltrated using a 1 mL syringe. Two days after infiltration, the leaves were either microscopically observed or used for protein isolation.

#### **Recombinant Protein expression and Purification, pull down assay**

The cDNA encoding the N-terminal of BrRbohF protein (BrRbohF-N, 1-345aa) were constructed into the PET-32a vector for His-tag fusion and expressed in E. coli BL21. Full-length cDNA fragment of BrROP2 was constructed into the PGEX-4T-1 vector for GST-tag fusion and expressed in E. coli BL21. The cDNA encoding the N-terminal of BrFER1 protein (BrFER1-N, 1-788 aa) were constructed into the pCXSN-56 vector for Myc-tag fusion and expressed in tobacco leaves by infiltration with Agrobacteria following the procedure described as above. For each expression vector, the insertion was confirmed using PCR and enzyme digestion, and sequence accuracy confirmed by Sanger sequencing. Full list of primers for RT-qPCR and for molecular clone was shown in Table S4.

For protein expression and purification, 100-200 mg tobacco leaves containing BrFER1-myc were grinded in liquid nitrogen, mixed in 1 mL extraction buffer in a 1.5 mL centrifuge tube and stayed on ice for 20 min. After centrifuge at 12000 rpm for 15 min at 4°C, the supernatant was transferred into a new centrifuge tube as total protein. BL21 cells containing BrROP2-GST or BrRbohF-N were induced using 1 mM IPTG at 37°C. The cells were spin down and the precipitate was resuspended with 5 mL PBS (140 mM NaCl, 2 mM KCl, 2 mM KH2PO4, 10 mM Na2HPO4·7H2O). After sonication (SCIENTZ JY92-IIN, China, voltage 220V, power 650W), the protein was purified by GSH-beads (BEAVER) or TALON beads (Clontech) as needed. The eluted proteins were electrophoresis separated by 10% SDS-PAGE and detected by the corresponding anti-body after western blot.

For pulldown assays, 50 µg purified protein was added to 50 µL of pre-washed GST magnetic beads (BEAVER) and incubated for 2h at RT. The beads were washed for 4 times, 5 min each time. The magnetic beads were mixed with 50 μL PBS with the SDS loading buffer and boiled for 5 min. After western blot, the protein was detected with the primary antibody (anti-GST/His/MYC antibody, 1:5000 in 5% milk, Abmart) and HRP conjugated secondary antibody (1:10000 in 5% milk, Abmart). The membrane was wash three times with TBST at 5 min interval and subjected to HRP detection kit (Vazyme) analysis with chemiluminescence imaging system (TIAN NENG, Beijing).

For Yeast two hybrid, full-length cDNA of BrROP2 and the cDNA encoding the N-terminal of BrRbohF protein (BrRbohF-N, 1-387 aa) or the C-terminal of BrRbohF (BrRbohF-C, 767-949 aa) were constructed into pGADT7 vector and pGBKT7 vector, 100 respectively. For Y2H, set up the following reaction: 100 uL Y<sub>2</sub>HGlod competent cells (TransGen Biotech), 2 μg BD plasmid, 10 μL pretreated Carrier DNA and 500 uL PEG/LiAc, mixed well. After heat shock treatment in the water bath at 42°C for 30 min, the cells were resuspended in 0.5 mL of sterile 0.9% NaCl and 100 μl cells were coated on SD/-Leu/-Trp agar plate for 2 days or SD/-Leu/-Trp/-His/-Ade plates and incubated at 30°C for 4 days. Pick several colonies from SD/-Leu/-Trp agar plate, streak on SD/-Leu/–Trp/–His/-Ade X-a-Gal agar plates, incubate at 30°C for days.

#### **QUANTIFICATION AND STATISTICAL ANALYSIS**

Bar graphs with dots were generated in Prism, bar graphs without dots were generated in Excel. Unless otherwise indicated, bar graphs or line graphs denote the mean, +/- s.d for all stigmatic ROS data, and ± sem for all the pollen tube growth data. Dots indicate each data point. n denotes the numbers of stigmas. Asterisks or n.s. directly above the data bars indicate significant difference (two-tailed t test, \*p < 0.05, \*\*p < 0.01) or no significant difference compared with the data bar on the far left, while \*\* or n.s. above the brackets show comparisons between the data bars as indicated. Each experiment was repeated at least three times with consistent results. Full information regarding the statistical analyses used in this study is shown in the legend of Figure 1 and also briefly mentioned in each figure legend.